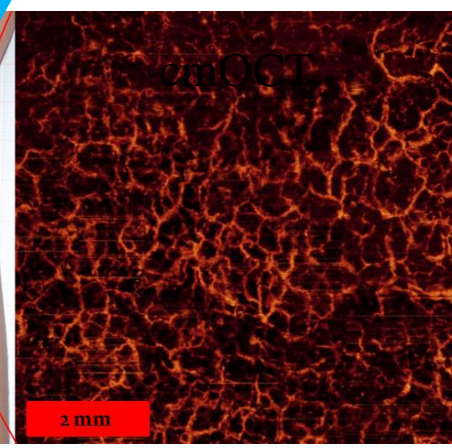
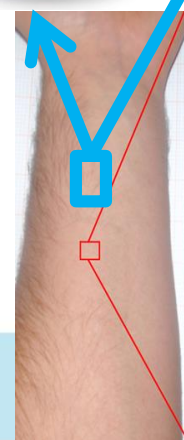
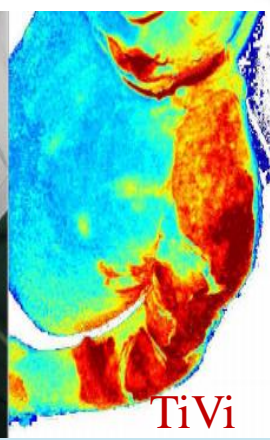
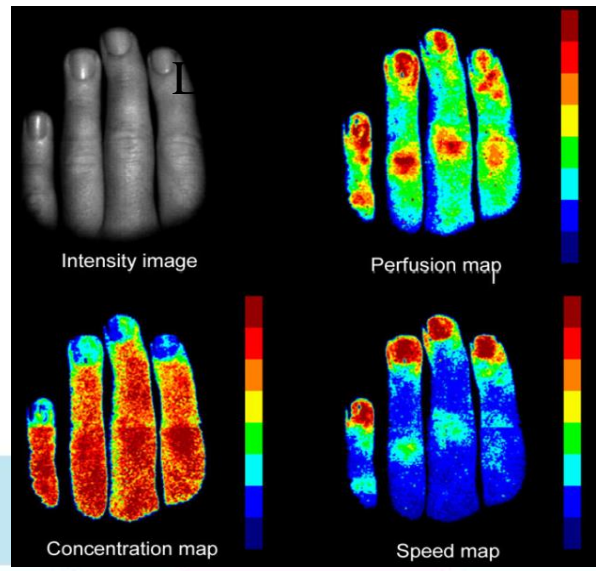
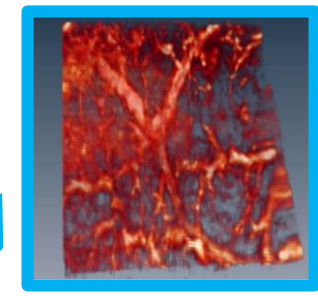
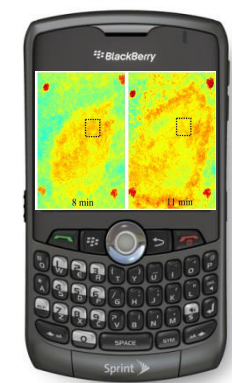
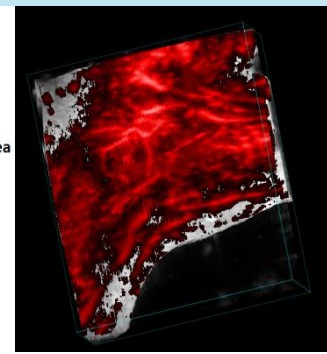
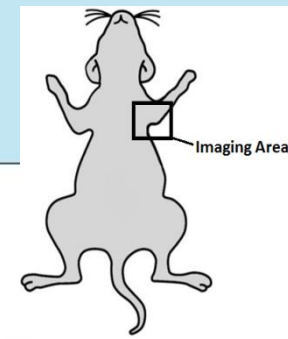
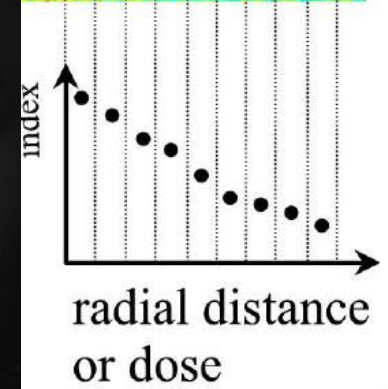
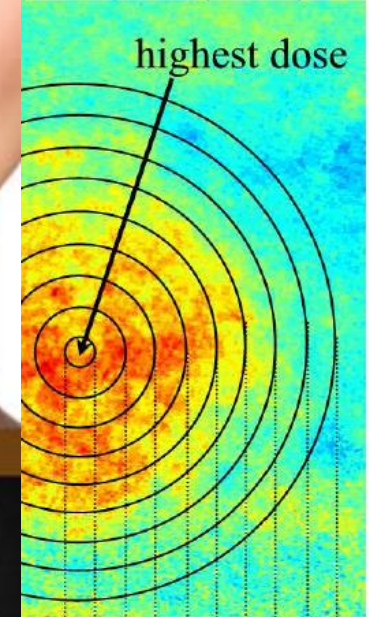


Microcirculation Imaging Techniques – TOMI lab

- Laser Doppler perfusion imaging (LDPI)
- Laser speckle contrast imaging (LSCI)
- Tissue viability imaging (TiVi)
- Photoacoustic Imaging (PAI)
- Optical coherence tomography (OCT)





O'Doherty, J., et al., 2011 .Arch Derm Res (2010)

Commercially available mHealth devices

Otoscope



Dermascope



Ophthalmoscope



Microscope

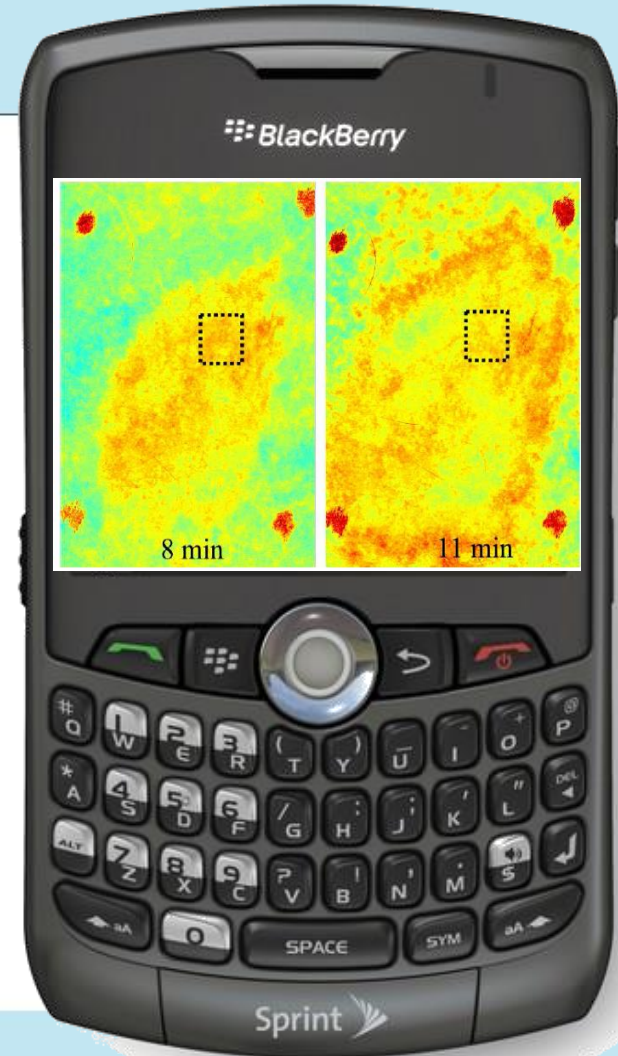
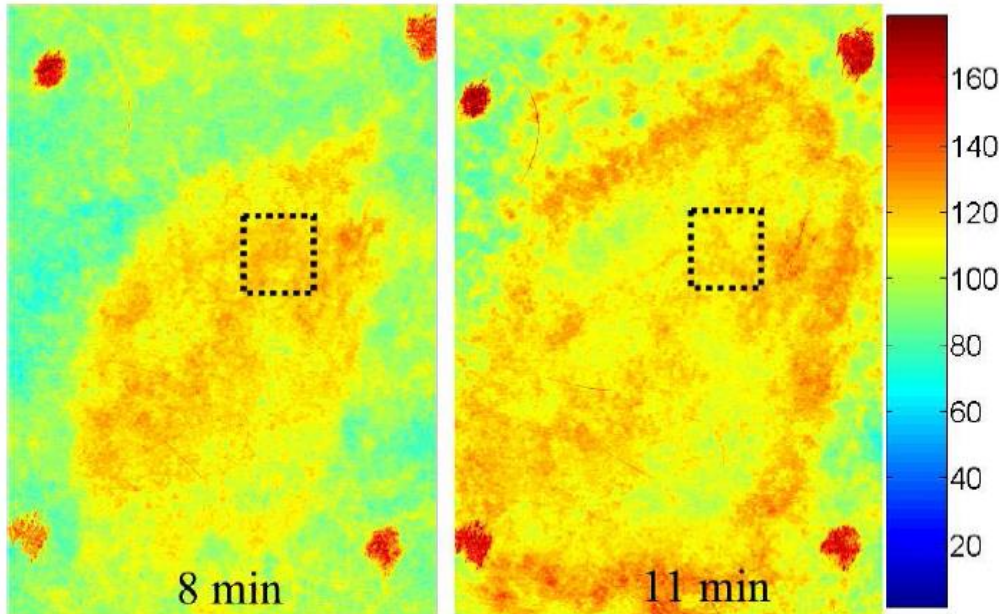


Ultrasound



Mobile platform

Swelling reduces TiVi index value
18% reduction in averaged value of
dashed box while the edges increase



J. Biophotonics 1–4 (2010) / DOI 10.1002/jbio.201000050.

J. Physiological Measurement (2010)



J. Biophotonics 1–4 (2010) / DOI 10.1002/jbio.201000050

Journal of
BIOPHOTONICS

LETTER

Cellular phone-based photoplethysmographic imaging

Enock Jonathan and Martin J. Leahy*

Tissue Optics and Microcirculation Imaging (TOMI) Facility, National Biophotonics
Department of Physics, University of Limerick, Ireland

Received 4 April 2010, revised 3 August 2010, accepted 3 August 2010
Published online 6 September 2010

Key words: photoplethysmography, biophotonics, optical imaging, cellular phone

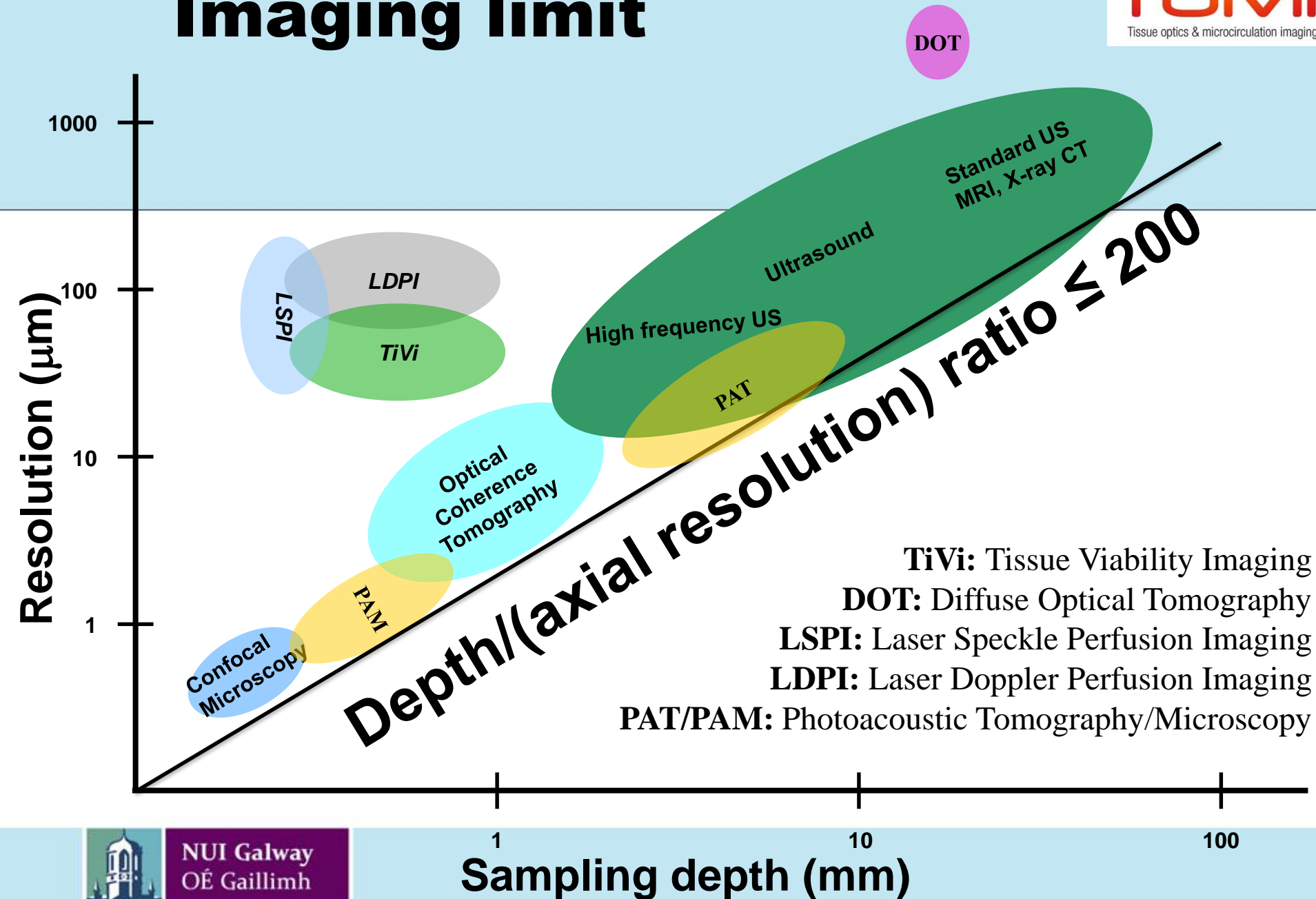
We present study results on visible light reflection photoplethysmographic (PPG) imaging with a mobile cellular phone operated in video imaging mode. PPG signal components around 0.1 Hz attributed to the sympathetic component of the heart rate, 1 Hz as the heart rate and 2 Hz as heart rate high order harmonic were quantified on the index finger of a healthy volunteer. The green channel reported PPG signals throughout the sampled area. The blue and red channel returned plethysmographic information, but the signal strength was highly position specific. Our results obtained with a cellular phone as the data acquisition device are encouraging, especially in the broad context of personal or home-based care and the role of cellular phone technology in medical imaging.



Spectral signature of Haemoglobin



Imaging limit



J. Biophotonics 1–4 (2010) / DOI 10.1002/jbio.201000050

Journal of
BIOPHOTONICS

LETTER

Cellular phone-based photoplethysmographic imaging

Enock Jonathan and Martin J. Leahy*

Tissue Optics and Microcirculation Imaging (TOMI) Facility, National Biophotonics
Department of Physics, University of Limerick, Ireland

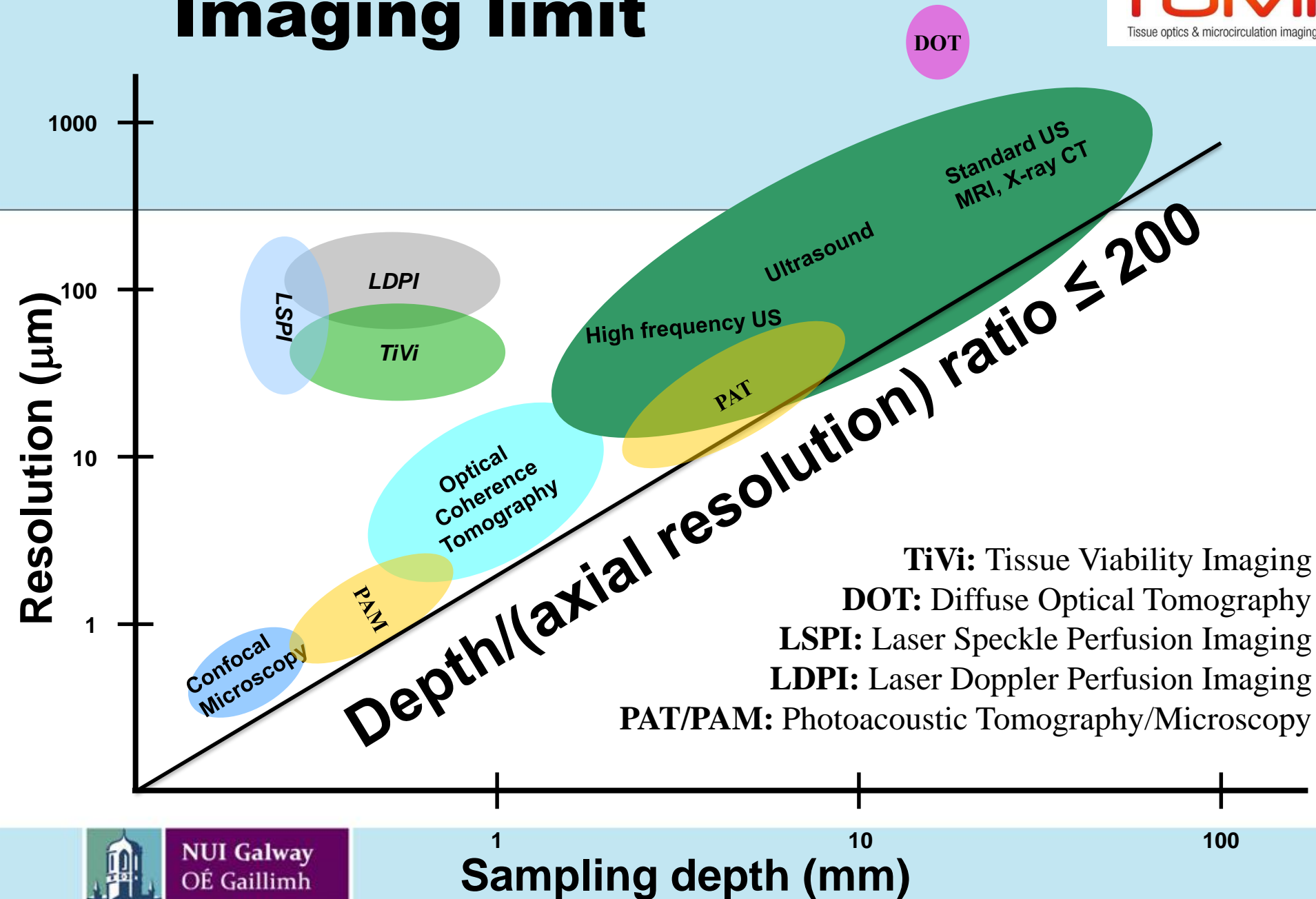
Received 4 April 2010, revised 3 August 2010, accepted 3 August 2010
Published online 6 September 2010

Key words: photoplethysmography, biophotonics, optical imaging, cellular phone

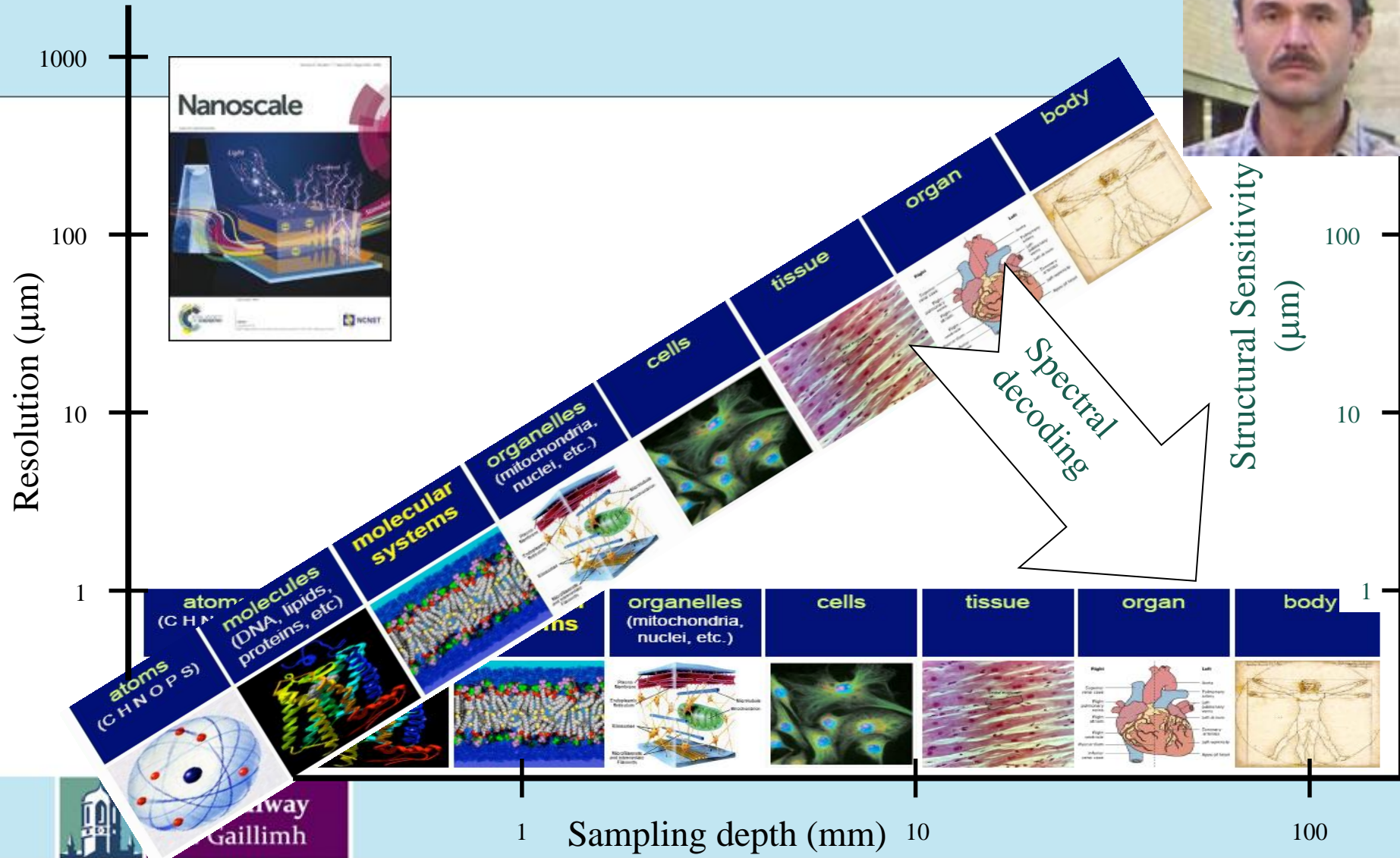
We present study results on visible light reflection photoplethysmographic (PPG) imaging with a mobile cellular phone operated in video imaging mode. PPG signal components around 0.1 Hz attributed to the sympathetic component of the heart rate, 1 Hz as the heart rate and 2 Hz as heart rate high order harmonic were quantified on the index finger of a healthy volunteer. The green channel reported PPG signals throughout the sampled area. The blue and red channel returned plethysmographic information, but the signal strength was highly position specific. Our results obtained with a cellular phone as the data acquisition device are encouraging, especially in the broad context of personal or home-based care and the role of cellular phone technology in medical imaging.



Imaging limit



Nanostructural sensitivity at depth



Home monitoring of retinal disease

- AMD^(a) and DR^(b) leading causes of blindness

- > 40 million cases in US and Europe alone
- Will double by 2020: demographics + diabetes



- Effective treatments exist, but burden huge and unsustainable

- All actors want clinical need for treatment to drive visit schedule
- However, after stabilization, necessary visit frequency varies by patient
- So, TAE protocols constrained by need to forestall events/treat quickly

- Critical need: *Home* monitor that provides clinically useful information

- Patients monitor as often as they want, reducing anxiety
- Doctors see patients when clinical need exists
- Unnecessary visits eliminated, reducing burden on all
- *And*, outcomes should improve

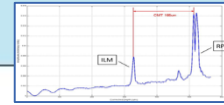


(a) Age-related macular degeneration
(b) Diabetic retinopathy



MR-OCT: one sensor, many applications

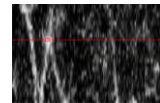
- Mobile health/fitness monitoring
 - Eye care/ophthalmology
 - Glucose concentration
 - Skin care/dermatology
 - Vital signs



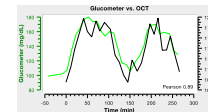
MR-OCT retinal thickness



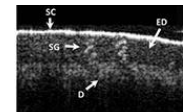
MR-OCT rat eye image



MR-OCT flow detection

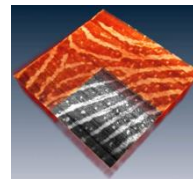


MR-OCT glucose tracking

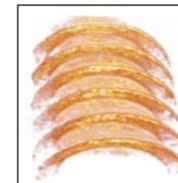


MR-OCT tissue image

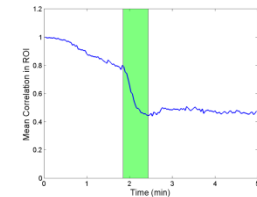
- Security and NDT (a)
 - Personal authentication
 - Document verification
 - Production testing



MR-OCT subdermal fingerprint

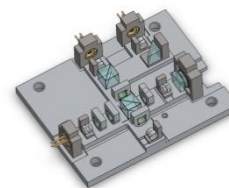


MR-OCT optical profiling



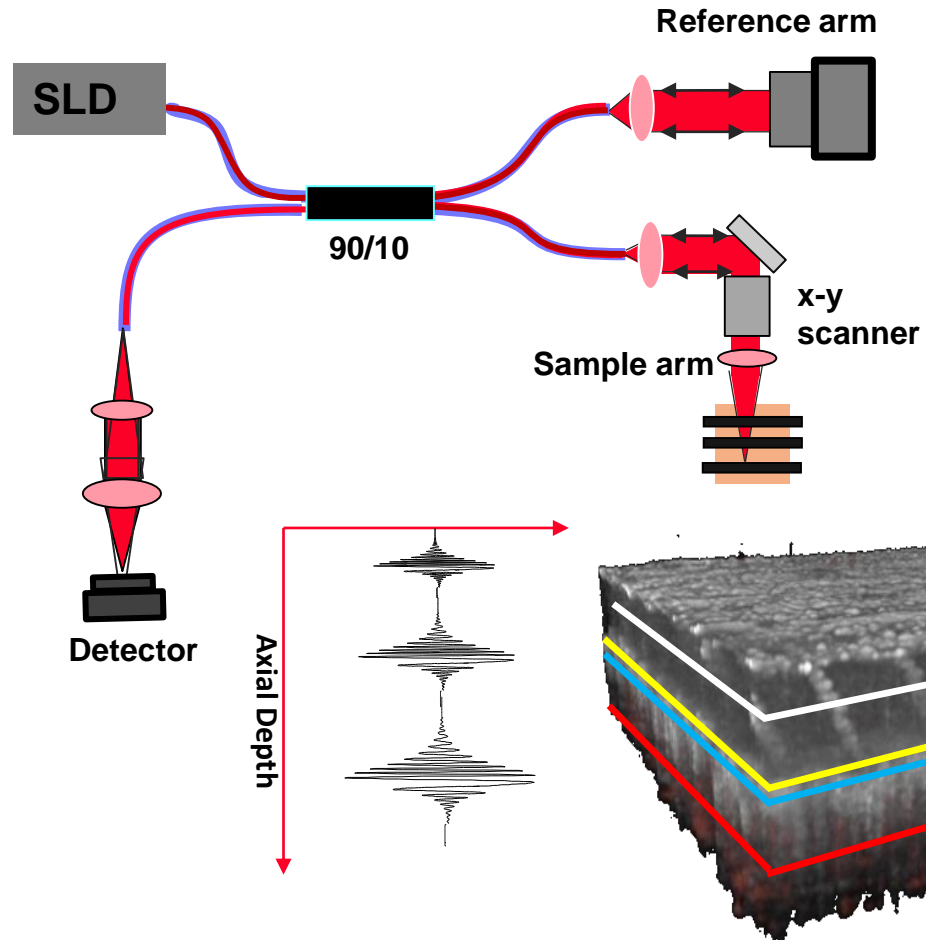
MR-OCT adhesive curing

- Key: MR-OCT suited to requirements
 - Noninvasive, subsurface
 - Sensitive, specific, fast
 - Small, low cost, battery power



Optical Coherence Tomography

- OCT uses low coherence interferometry to produce a two or three dimensional image of optical scattering from internal tissue microstructures.
- OCT can provide both micro structural and functional information with high resolution and sensitivity
 - High resolution (2-15 μm)
 - 3D imaging in scattering tissue (2-3 mm)
 - Non invasive – “Optical Biopsy”



Commercially available OCT systems

Cirrus HD-OCT



ILUMIEN



Skintell

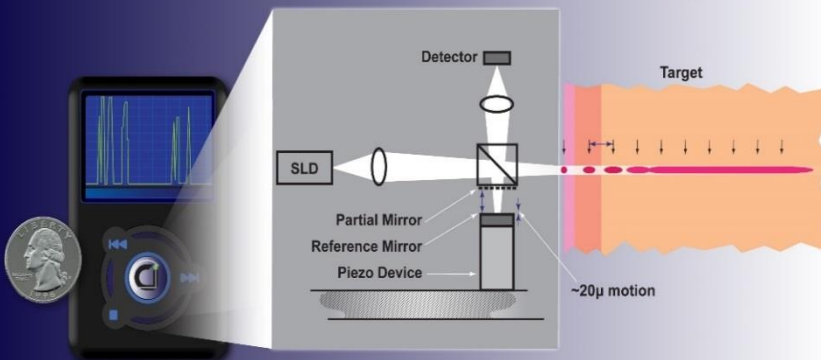


Conventional clinic-scale OCT instruments, priced from €45,000 to over €120,000, were commercialized early in the last decade for use by ophthalmologists, dermatologist, cardiac surgeons

Compact imaging solution with MR-OCT

Compact Imaging *MRO*TM Architecture

• Partial mirror combined with piezo-mounted reference mirror generates multiple OCT scans of increasing length simultaneously at different depths in target

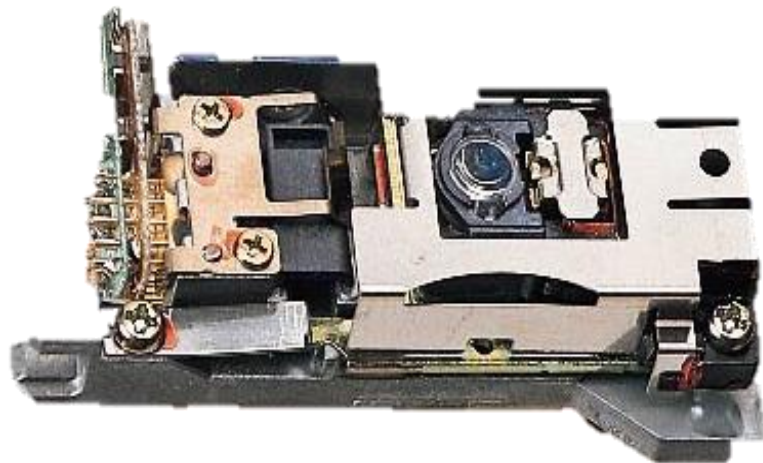


• Same combination enables compact solution

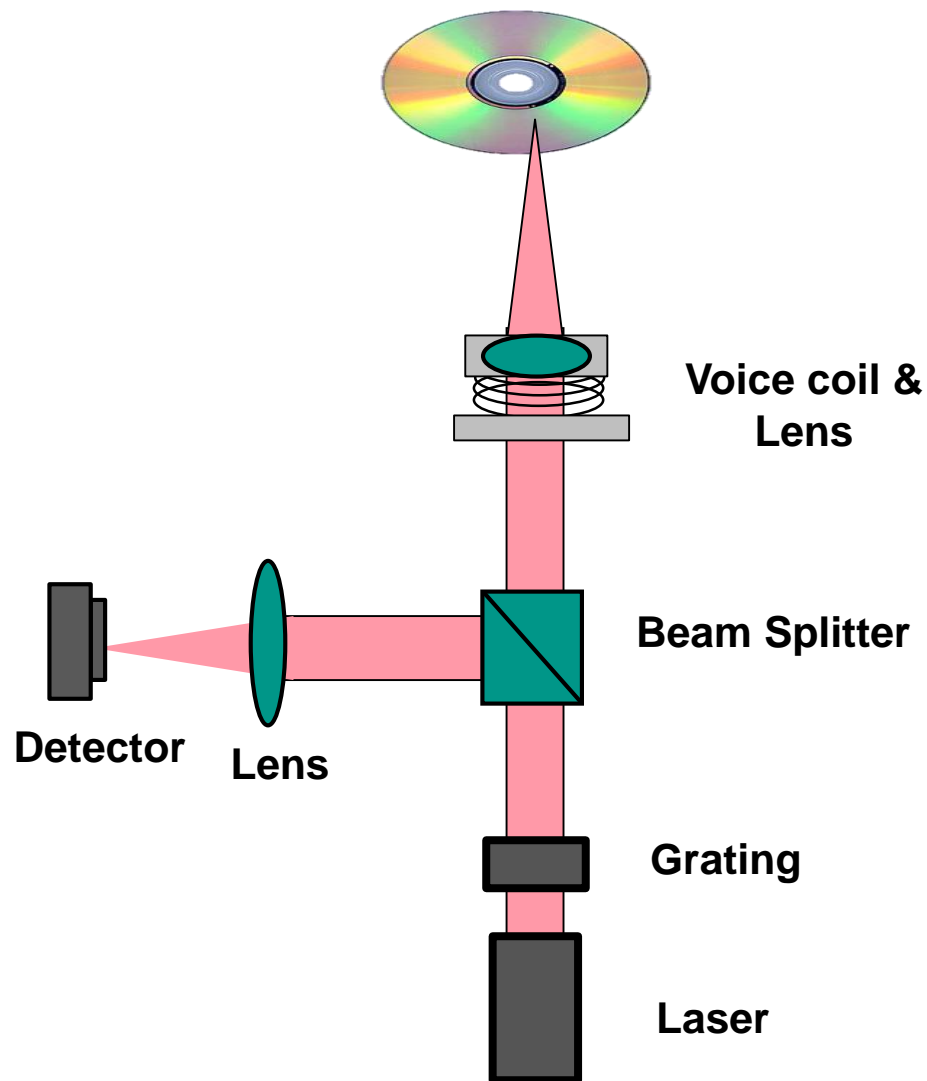
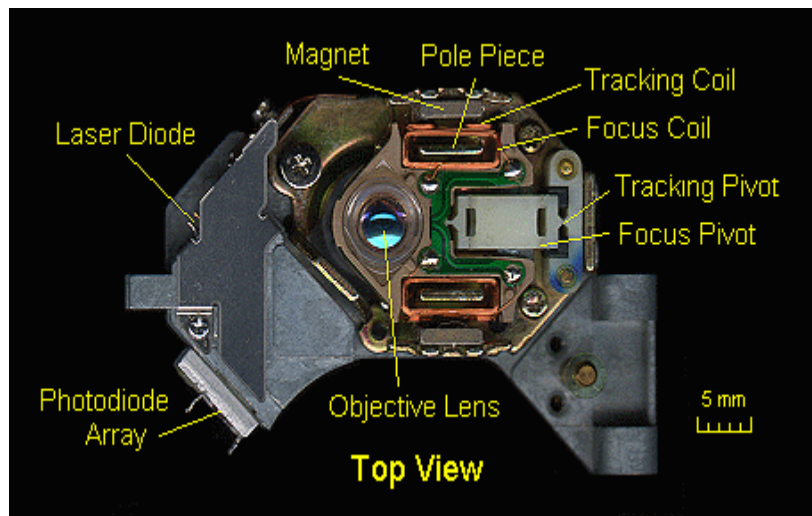
MR-OCT features

- Small form factor: About the size of a computer DVD read/write head
- Robust, cost-effective design: Virtually solid state, typical of handheld devices
- Low-operating power requirements
- Flexible “free space” optical architecture

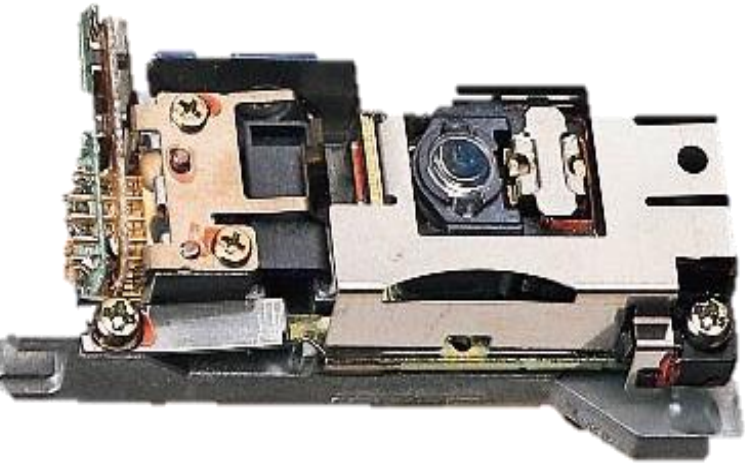
CD ROM Pickup Unit



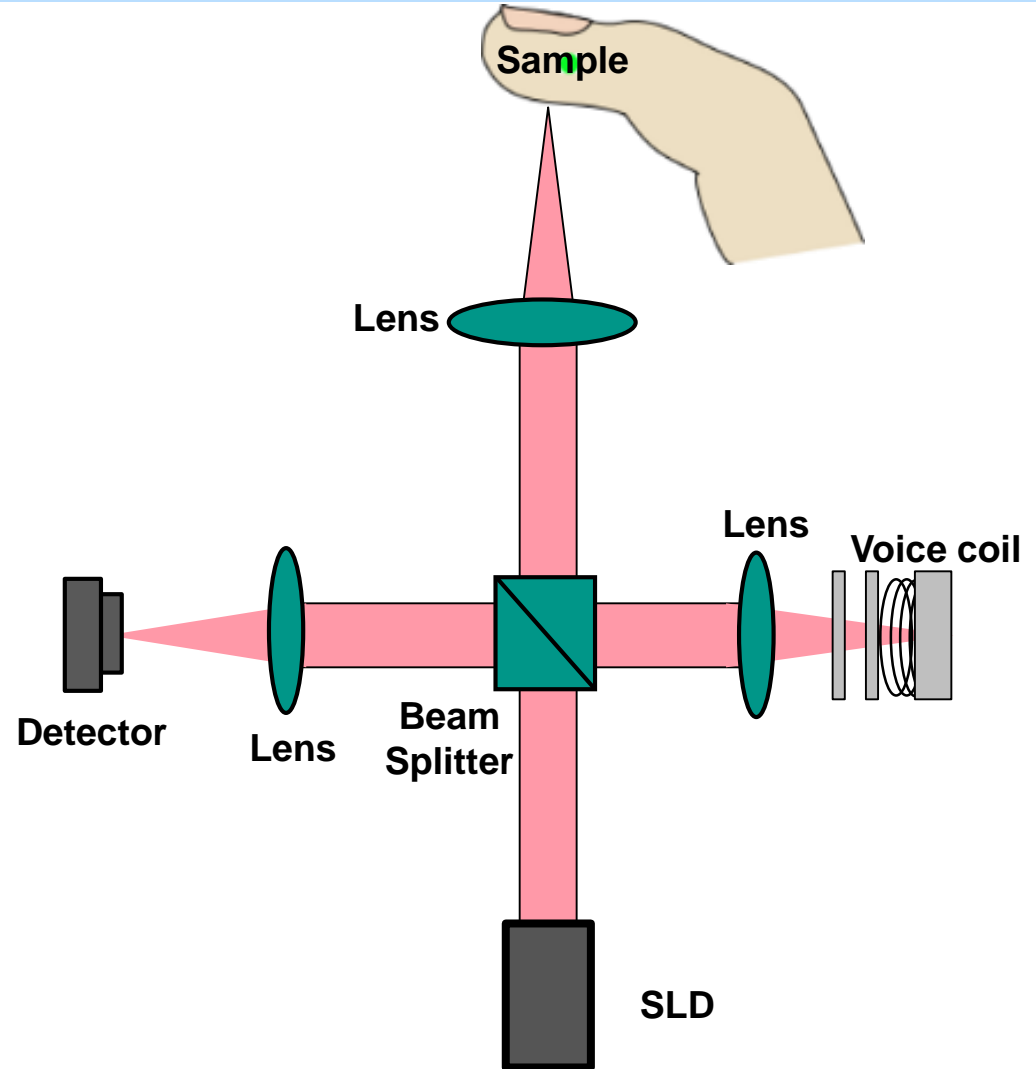
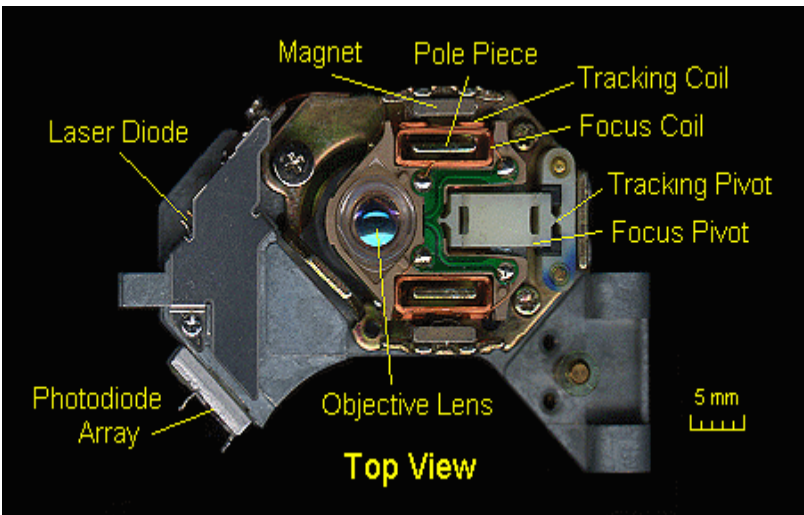
Cost 10\$!!!



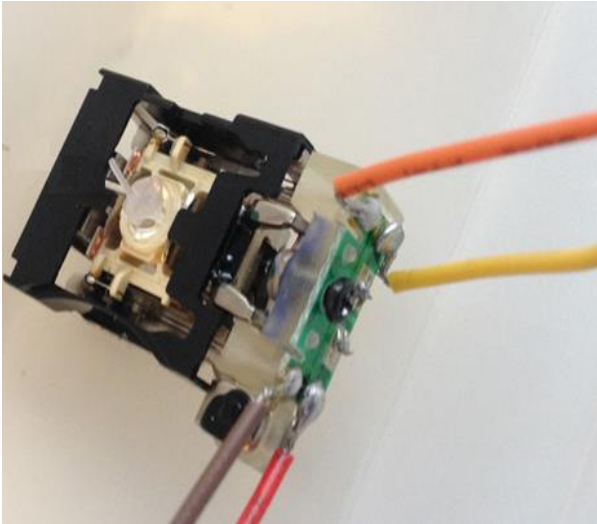
Replacing CD ROM Pickup Unit with MR-OCT



Cost 10\$!!!



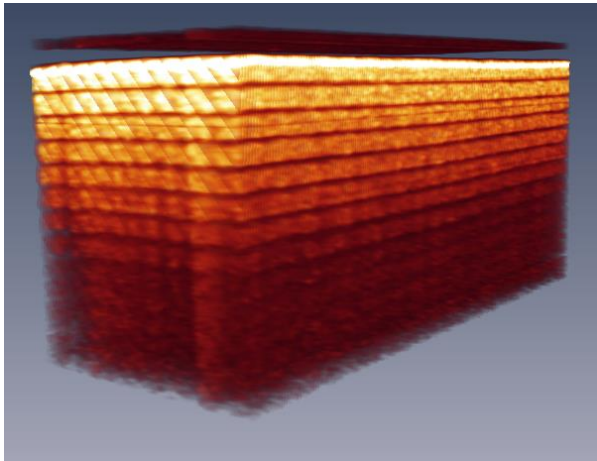
CD ROM Pickup head actuator



Voice coil motor (VCM) actuator used in CD pick up head to ensure the constant focus on the optical disc

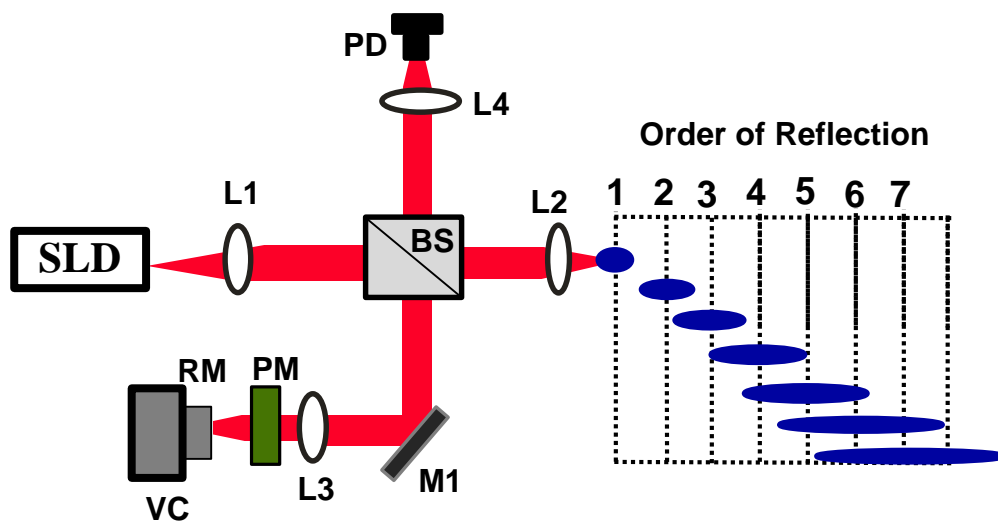
Voice coil features

- Low operational voltage
- Long life
- Light weight
- Inexpensive

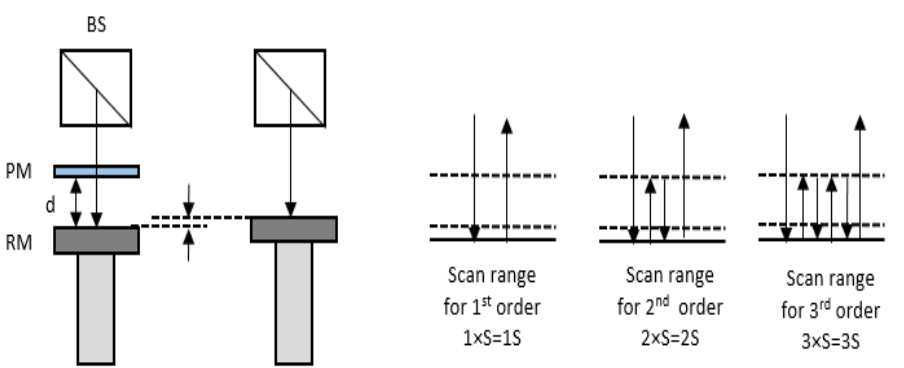


MR-OCT of Scotch tape with VCM

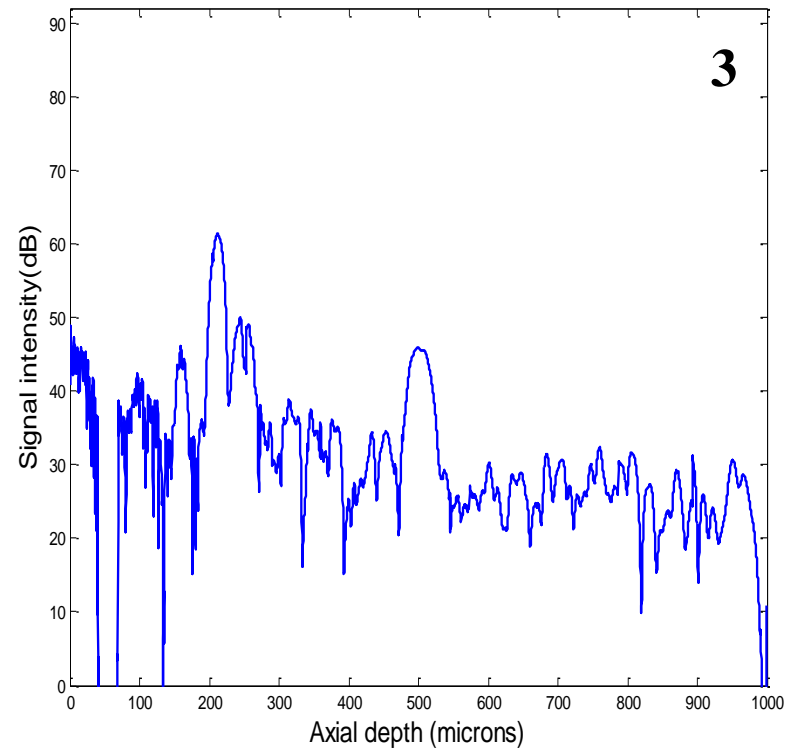
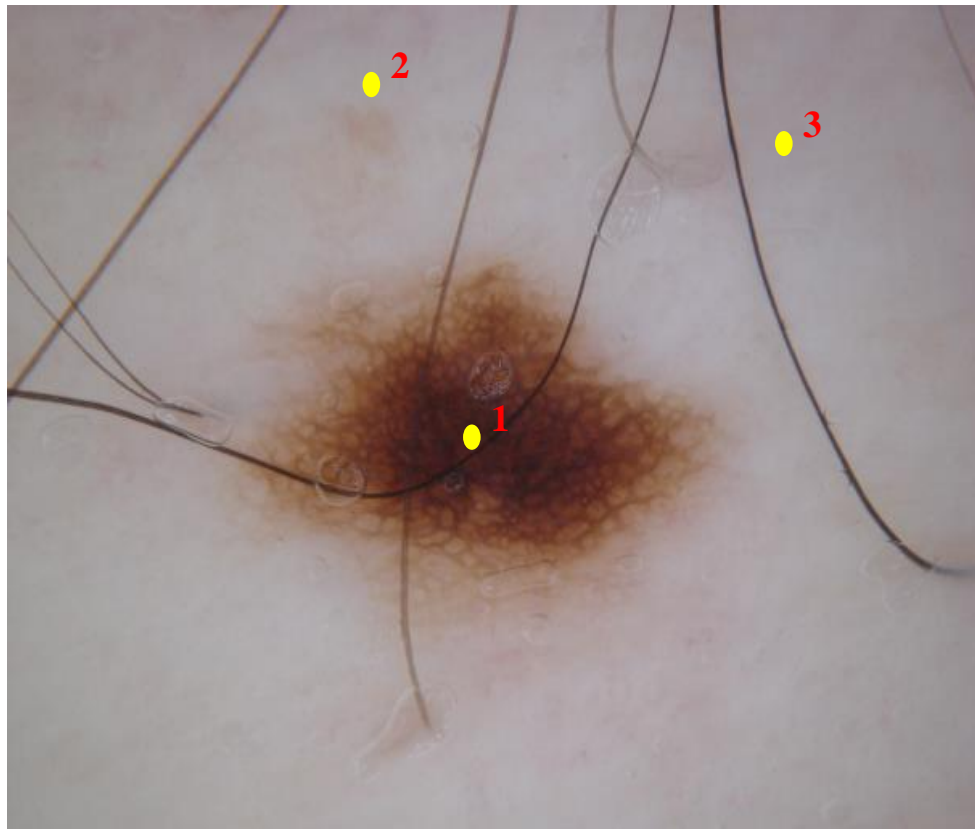
Multiple Reference Optical Coherence Tomography (MR-OCT)



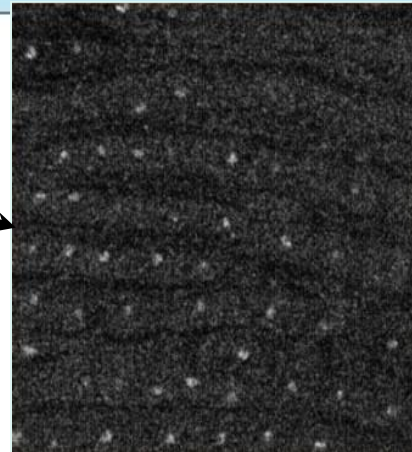
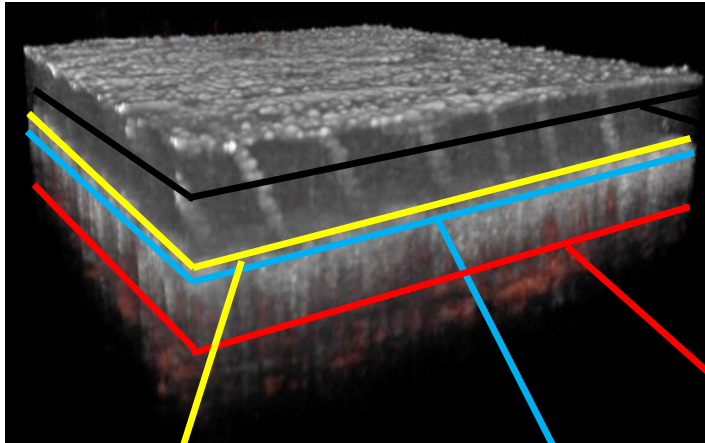
- MR-OCT is similar to conventional TD-OCT, except a partial mirror is placed very close to the reference mirror.
- The partial mirror causes the light to be reflected back and forth multiple times between the partial mirror and the reference mirror.
- Each reflection between the partial and reference mirrors is delayed by the round trip time between the two mirrors.



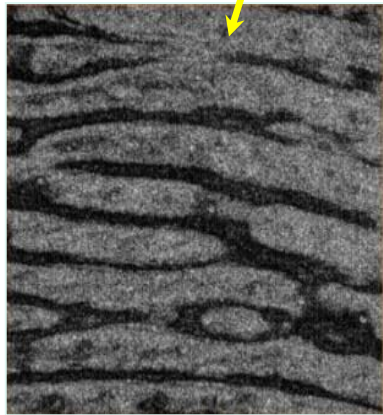
Co-registering MR-OCT beam with dermascope image



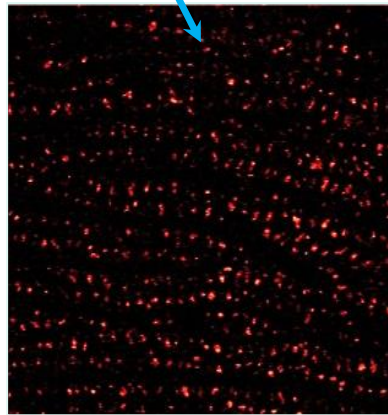
cmOCT of the thumb for a 5x5x3 mm region



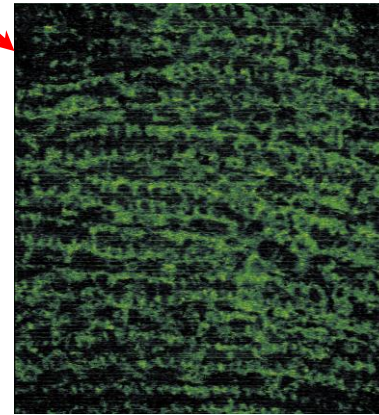
Sweat ducts



Sub-surface Fingerprint



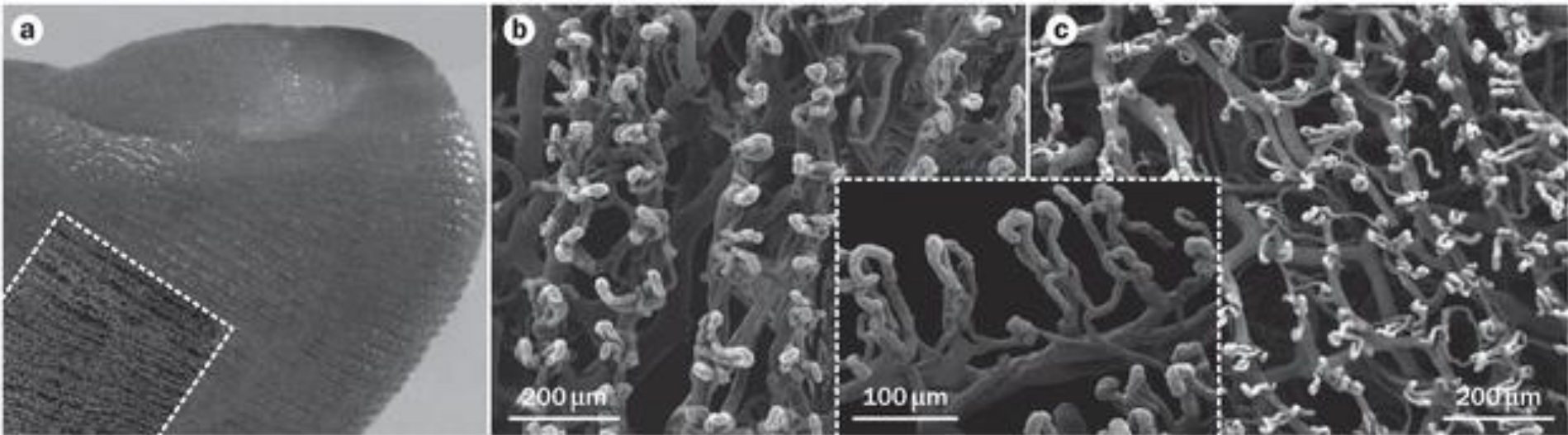
Rising Capillary Loops



Microcirculation Map



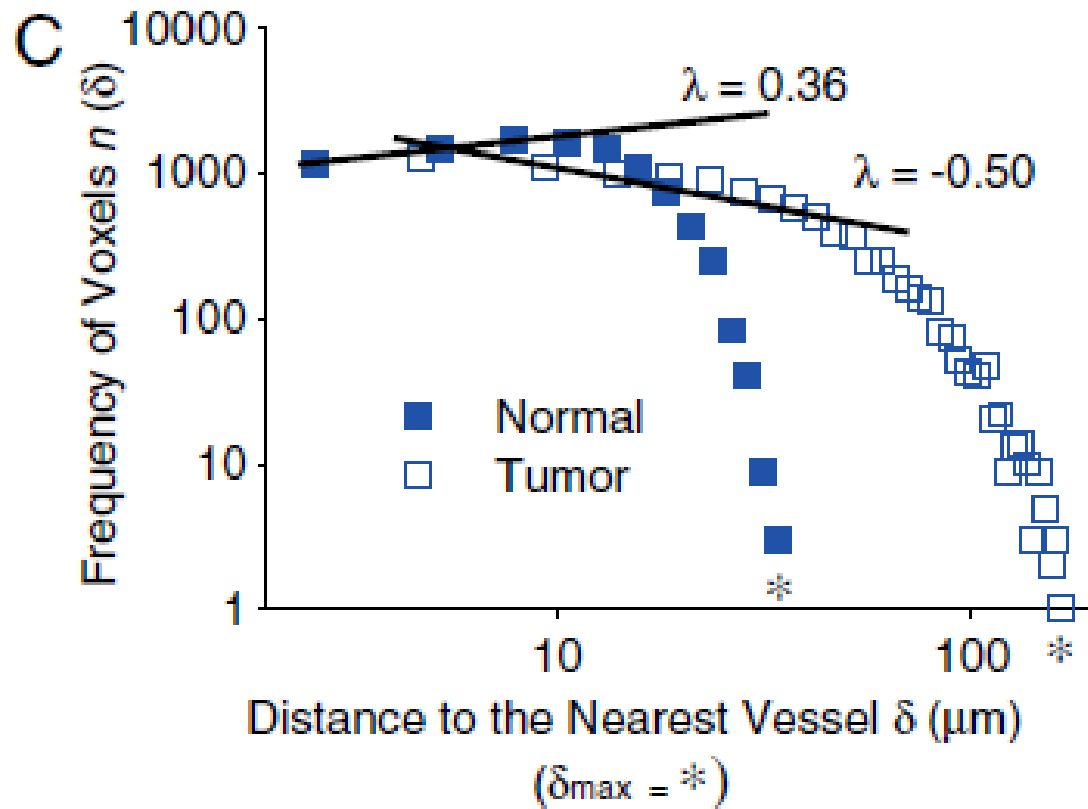
Fingerprint Microcirculation



Nature Reviews | **Rheumatology**



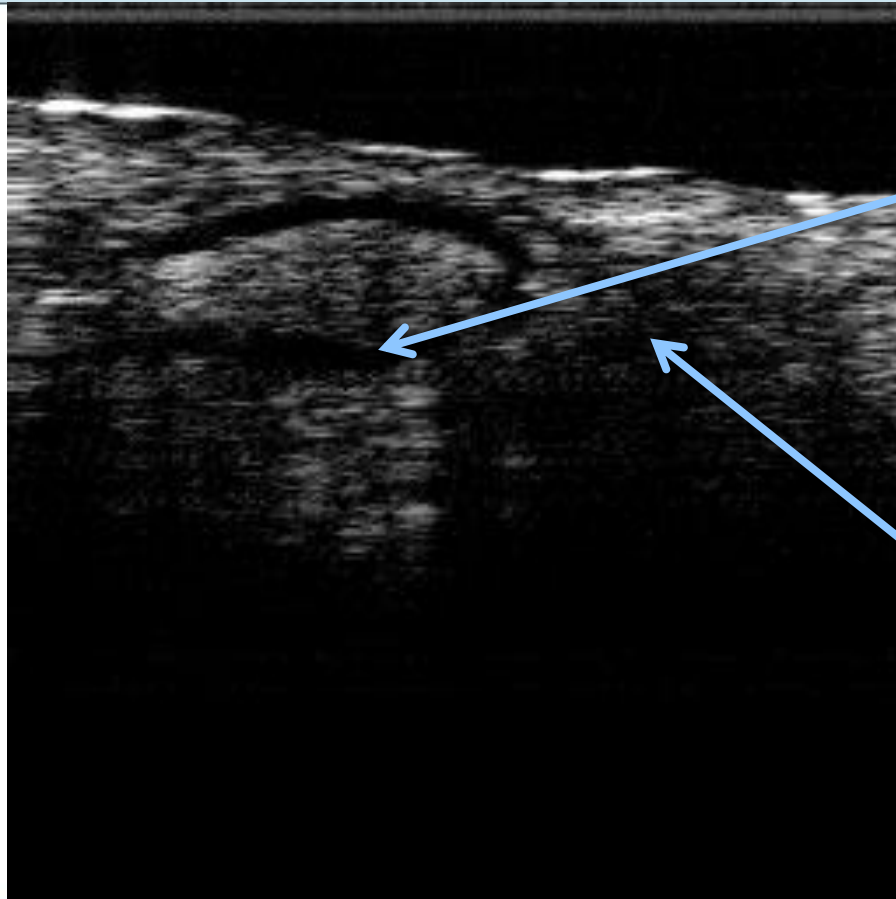
Scaling rules for diffusive drug delivery in tumor and normal tissues



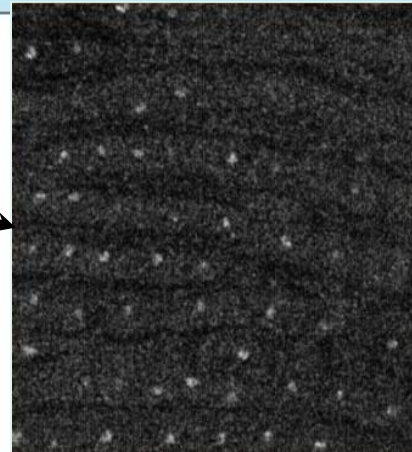
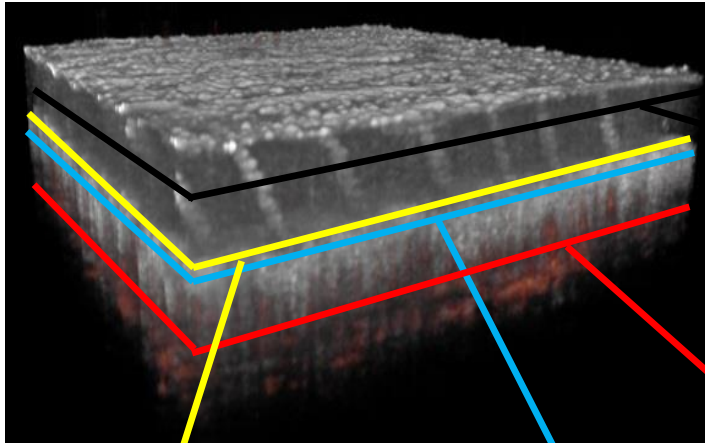
Principle of cmOCT

200 μm embedded capillary tube with flowing fluid

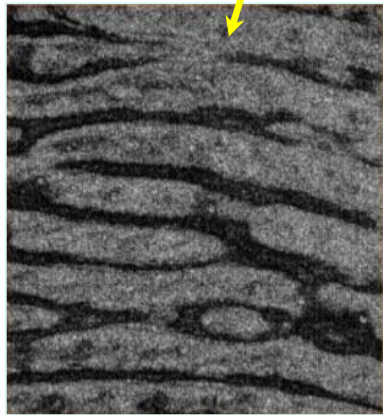
Excised section of Pig Skin



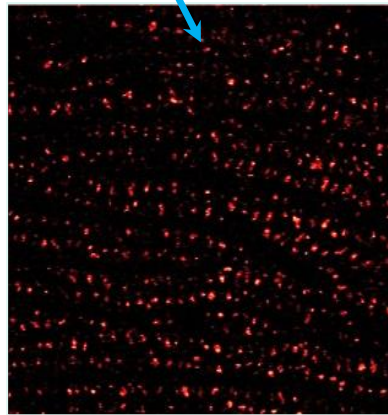
cmOCT of the thumb for a 5x5x3 mm region



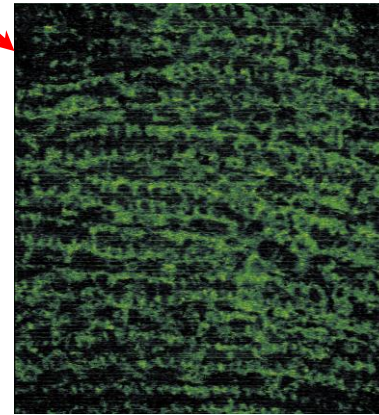
Sweat ducts



Sub-surface Fingerprint



Rising Capillary Loops

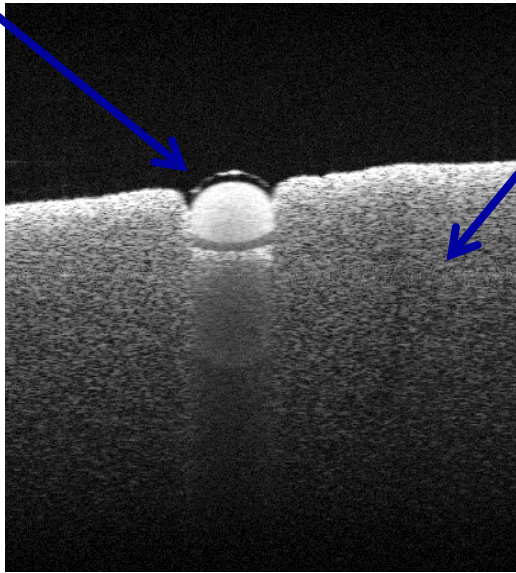


Microcirculation Map

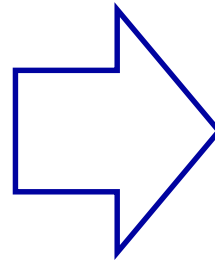


Correlation mapping OCT (cmOCT): Principle

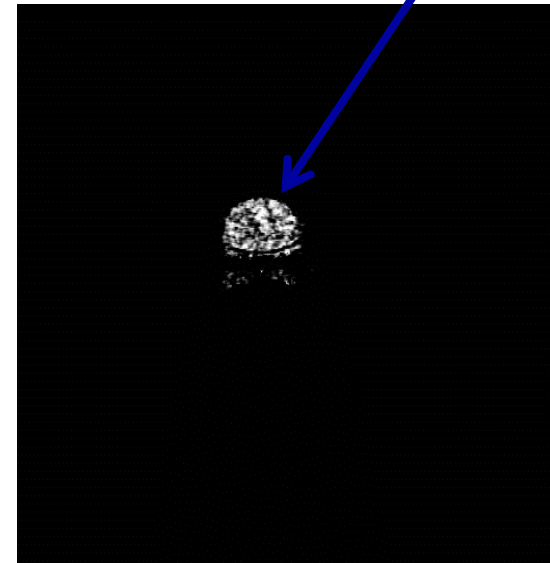
Flow region



Static region



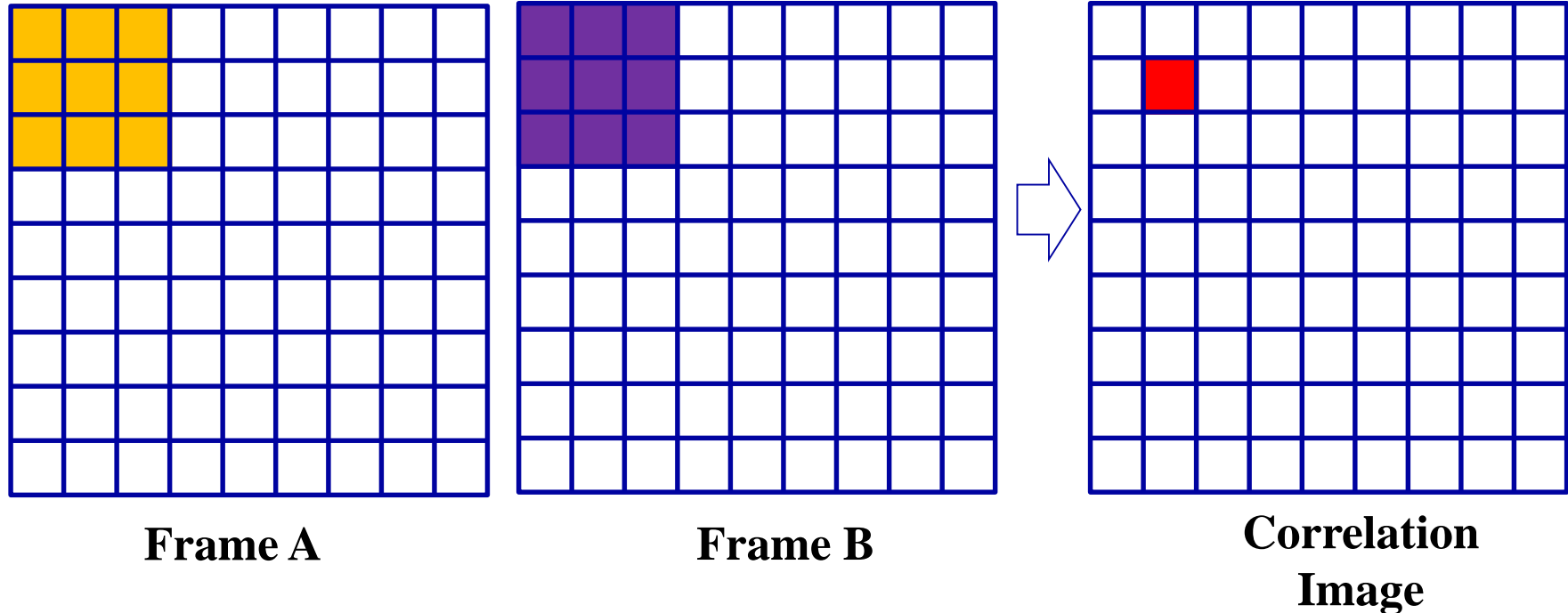
Flow region



Joey Enfield, Enock Jonathan, and Martin Leahy, "In vivo imaging of the microcirculation of the volar forearm using correlation mapping optical coherence tomography (cmOCT)," Biomed. Opt. Express 2, 1184-1193 (2011)



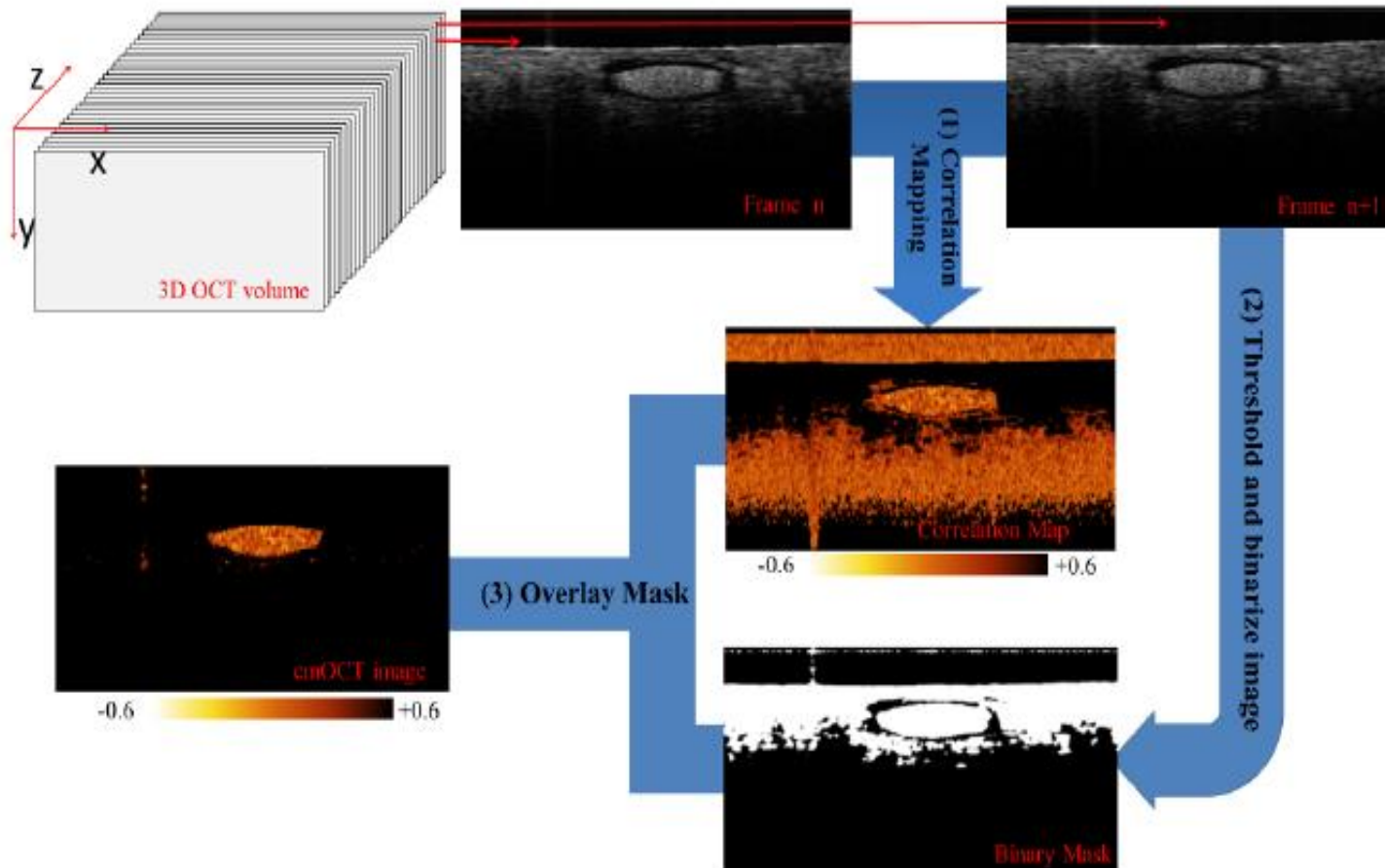
Correlation mapping OCT (cmOCT): Principle



$$cc(x, z) = \sum_{p=0}^M \sum_{q=0}^N \frac{[I_A(x+p, z+q) - \bar{I}_A(x, z)] [I_B(x+p, z+q) - \bar{I}_B(x, z)]}{\sqrt{[I_A(x+p, z+q) - \bar{I}_A(x, z)]^2 [I_B(x+p, z+q) - \bar{I}_B(x, z)]^2}}$$

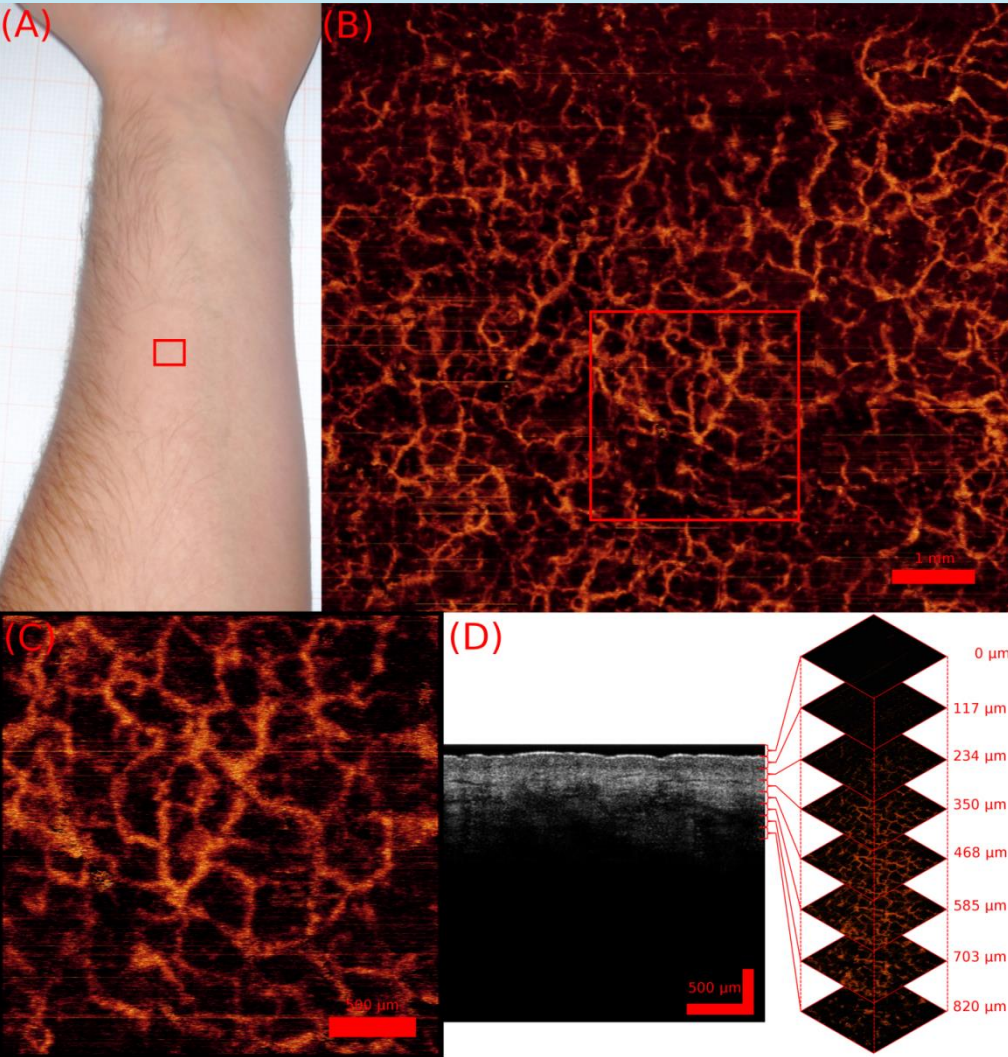
Where M, N are the grid size

Correlation mapping OCT (cmOCT): Principle



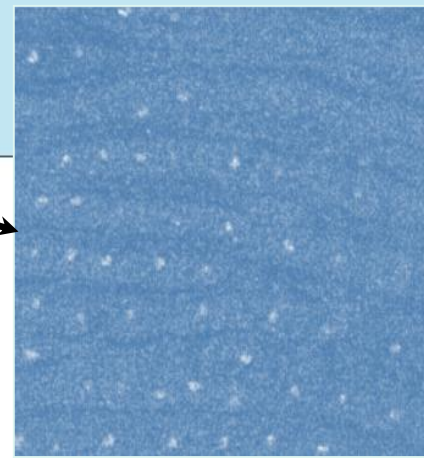
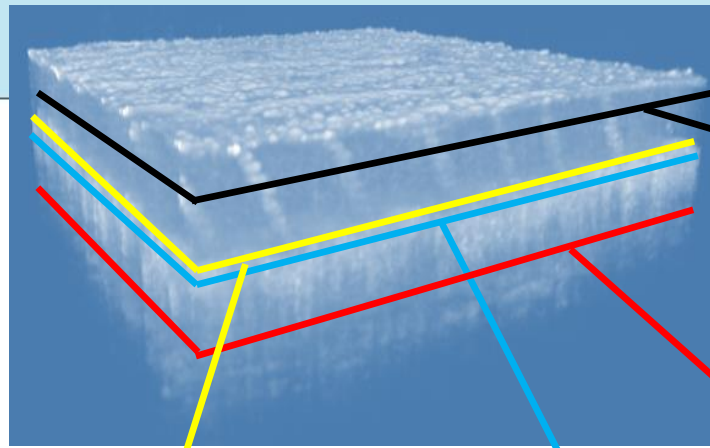
Joey Enfield, Enock Jonathan, and Martin Leahy, "In vivo imaging of the microcirculation of the volar forearm using correlation mapping optical coherence tomography (cmOCT)," *Biomed. Opt. Express* 2, 1184-1193 (2011)

cmOCT

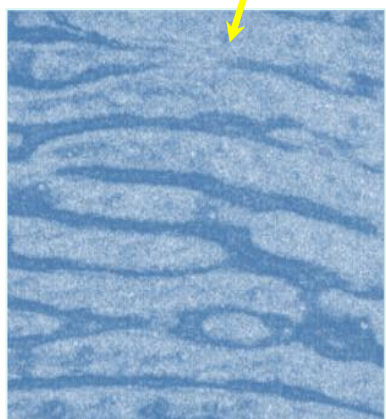


- Correlation mapping OCT
- 8 sequential frames
- 2-D correlation map average correlation value for a square grid measuring 7x7

Results: cmOCT of the thumb for a 5x5x3 mm region



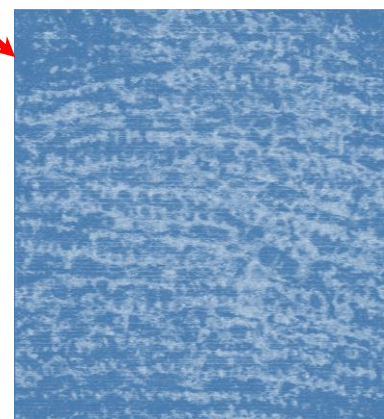
Sweat ducts



Sub-surface Fingerprint



Rising Capillary Loops



Microcirculation Map

Zam et al., 2013. *J. Biophoton.* **6** (9), 663-667.
McNamara et al., 2014. *J. Biomed. Opt.* **18** (12), 126008

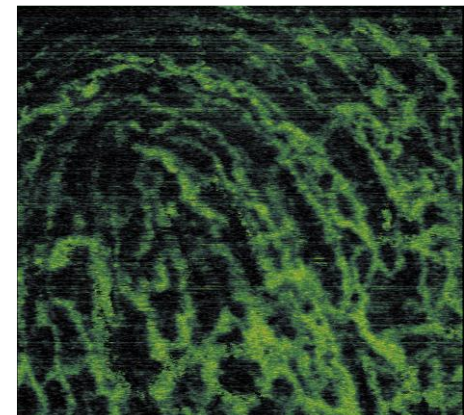
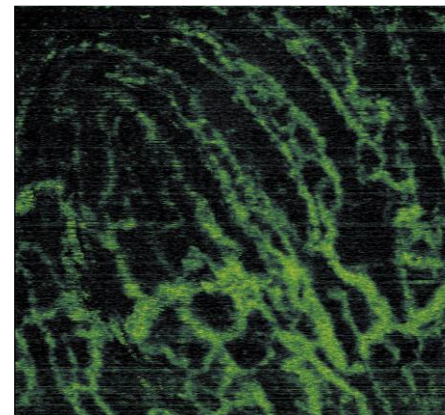
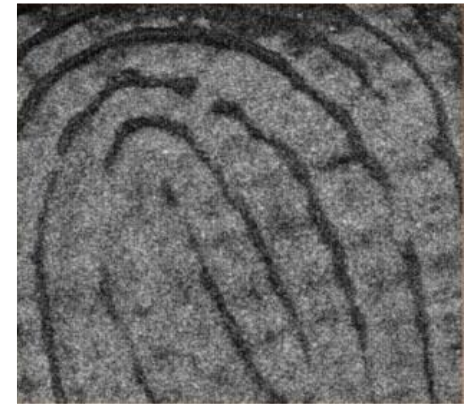
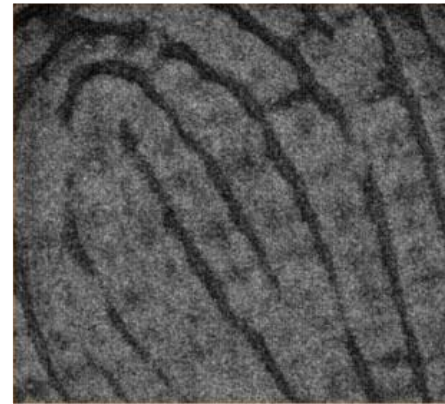
Secure biometric access to smartphones



Middle finger

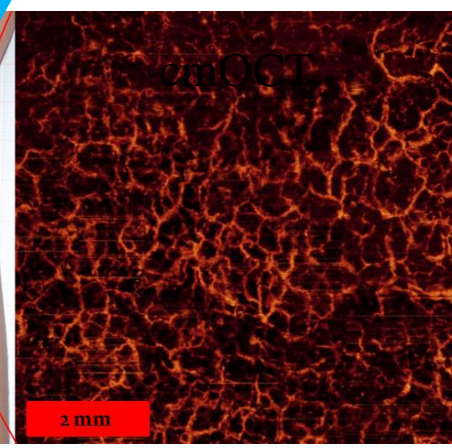
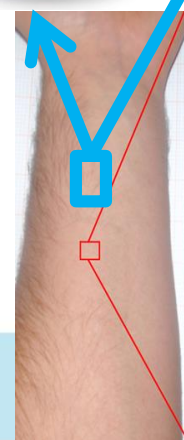
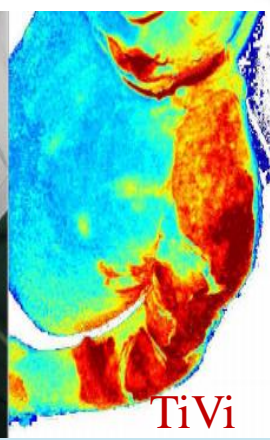
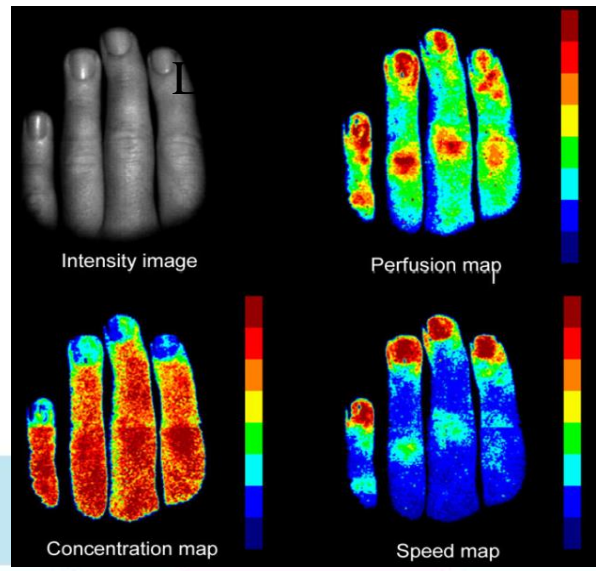
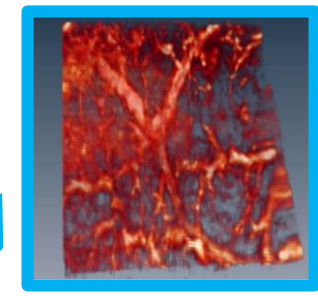
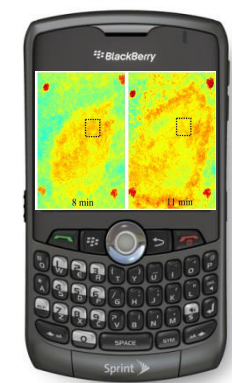
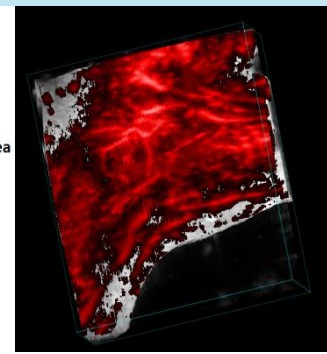
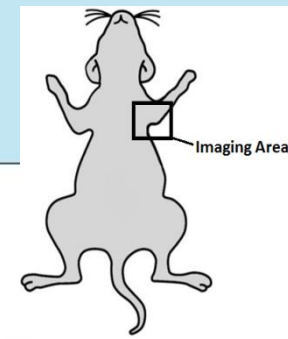
Day 1

Day 30



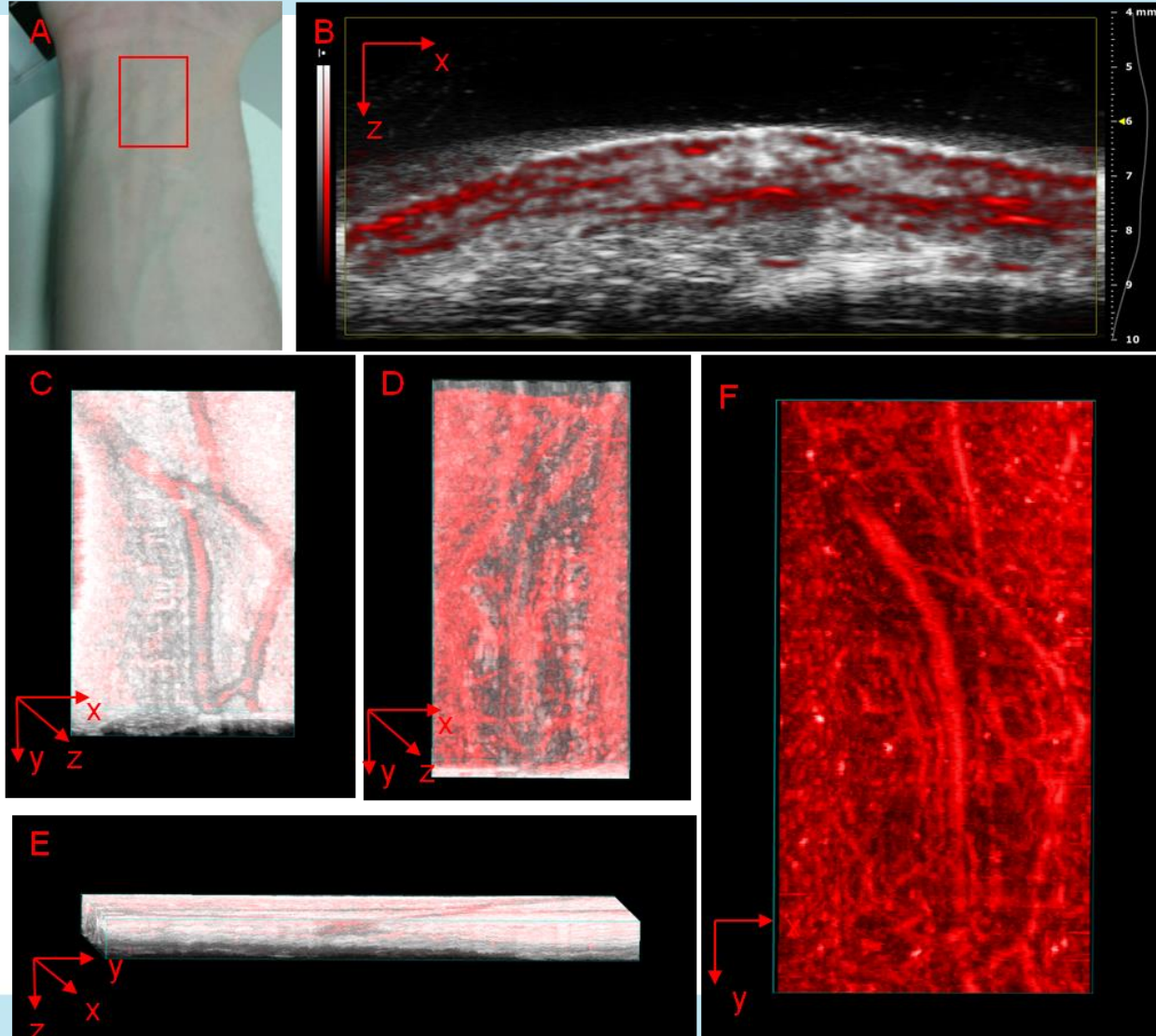
Microcirculation Imaging Techniques – TOMI lab

- Laser Doppler perfusion imaging (LDPI)
- Laser speckle contrast imaging (LSCI)
- Tissue viability imaging (TiVi)
- Photoacoustic tomography (PAT)
- Optical coherence tomography (OCT)



In vivo imaging of human forearm using 40 MHz transducer

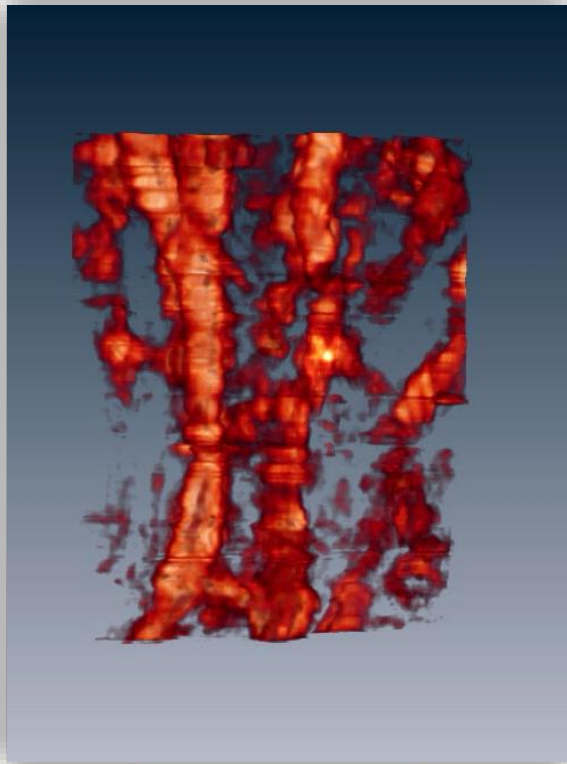
- In vivo PA and high frequency ultrasound images of the human forearm for a 30.5 (length) x 14.1 (width) x 10 (depth) region using 40 MHz probe at 860 nm.



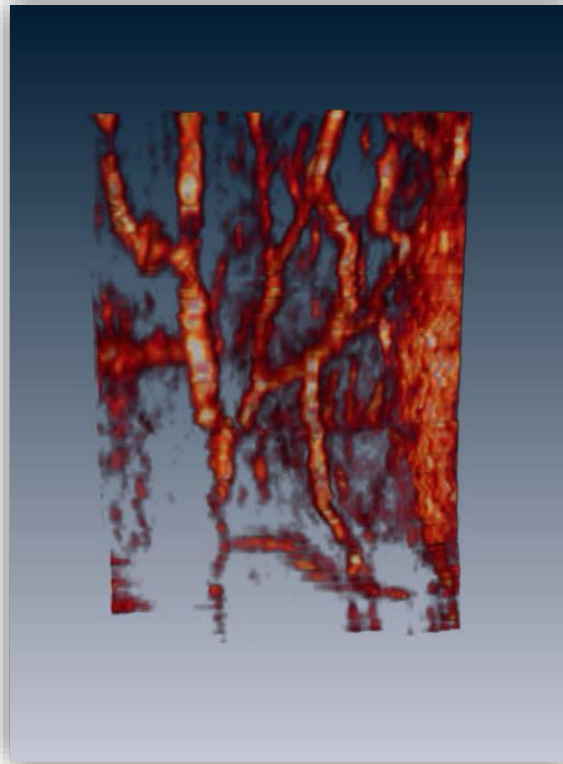
Comparison of 15, 21 & 40 MHz transducers

- Comparison of *in vivo* images of the human forearm acquired at the same location using 15 MHz, 21 MHz and 40 MHz transducer probes at 1064 nm.

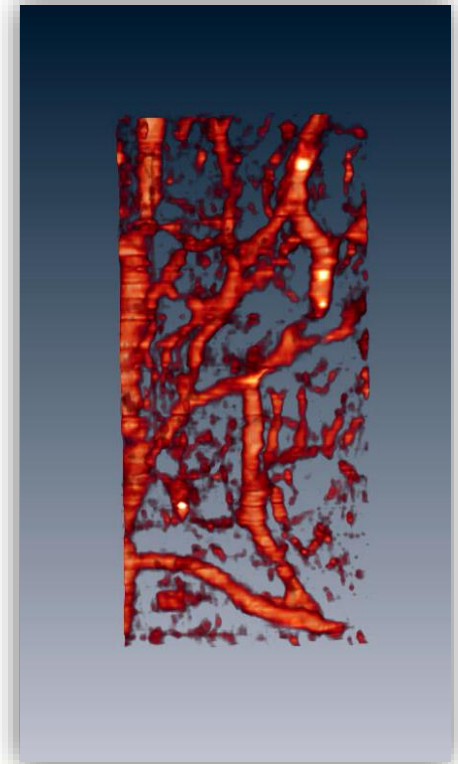
15 MHz (rendered)
30.5 mm x 23 mm (l x w).



21 MHz (rendered)
30.5 mm x 23 mm (l x w).



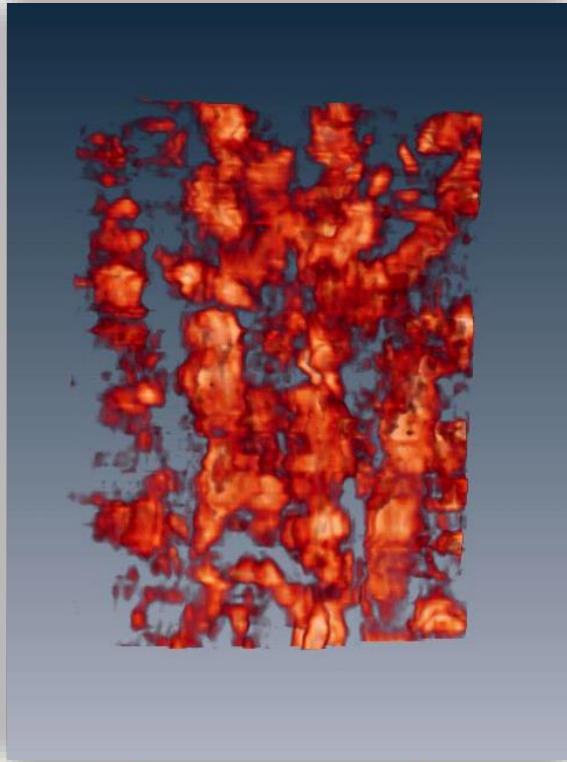
40 MHz (rendered)
30.5 mm x 14 mm (l x w).



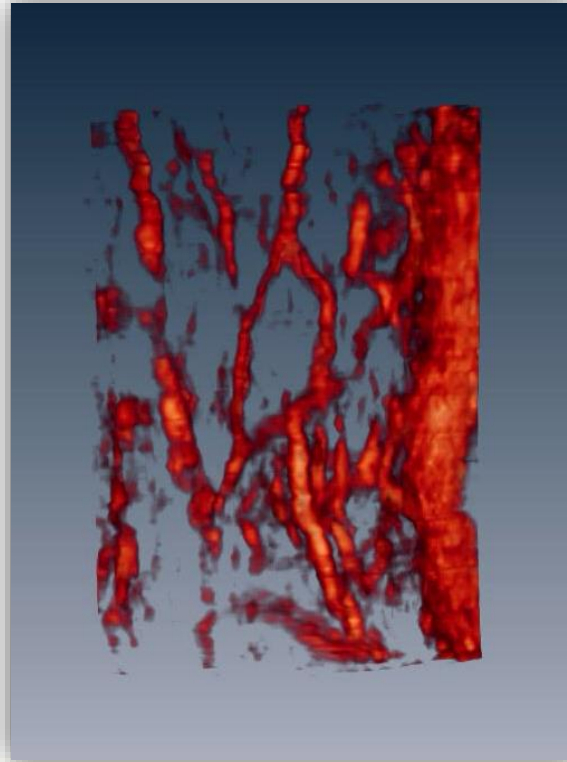
Comparison of 15, 21 & 40 MHz transducers

- Comparison of *in vivo* images of the human forearm acquired at the same location using 15 MHz, 21 MHz and 40 MHz transducer probes at 800 nm.

15 MHz (rendered)
30.5 mm x 23 mm (l x w).



21 MHz (rendered)
30.5 mm x 23 mm (l x w).

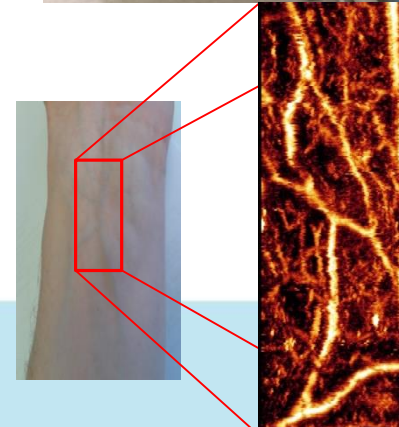
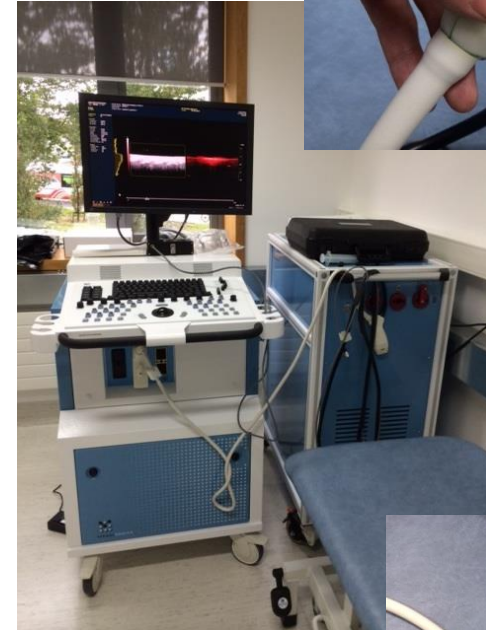


40 MHz (rendered)
30.5 mm x 14 mm (l x w).

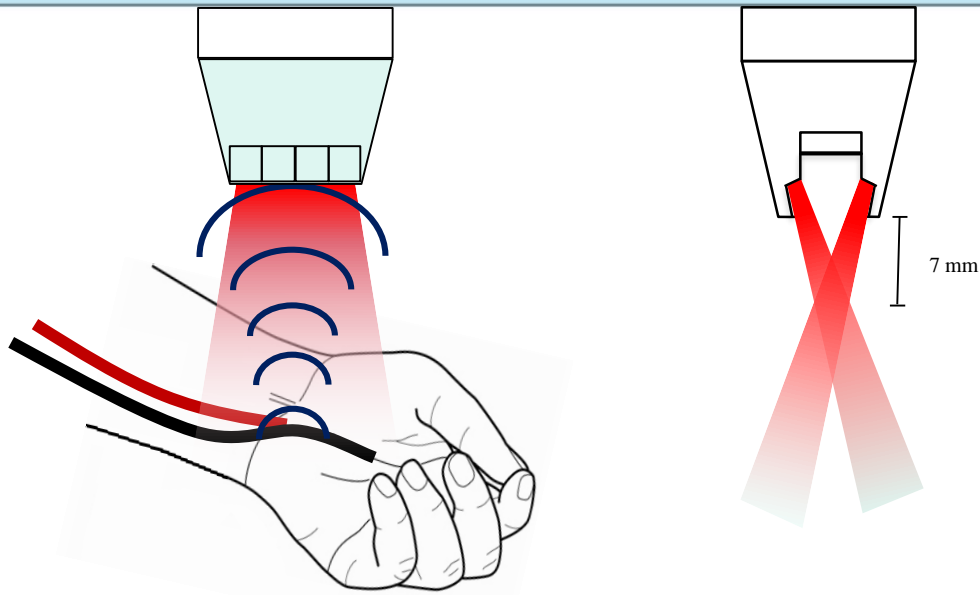


Visual Sonics Vevo® LAZR PAI System

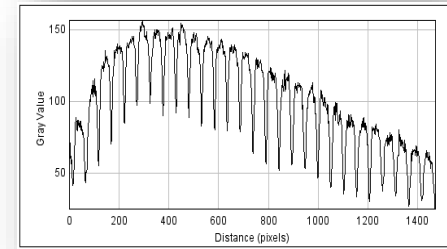
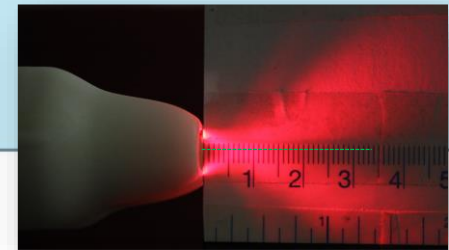
- OPO pumped by doubled Nd:YAG 680-970 nm, 20 Hz repetition rate, 5 ns pulse width, 45 +/- 5 mJ pulse energy
- 532 nm, 680-970 nm, 1064 nm, and 1200-2000 nm
- Real-time coregistered US and PA images
- Laser light delivery and Ultrasound (US) detection in single PA probe



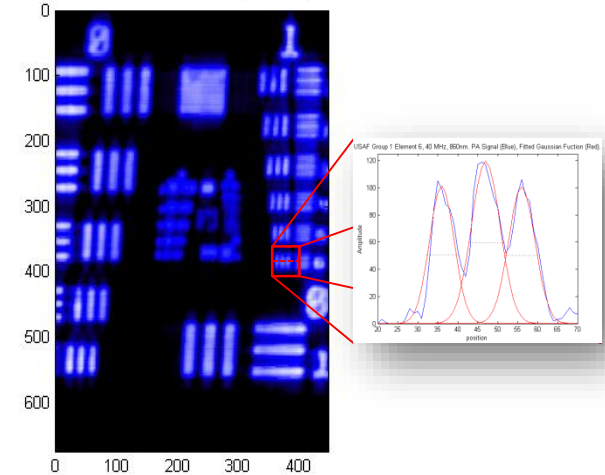
40 MHz PA probe



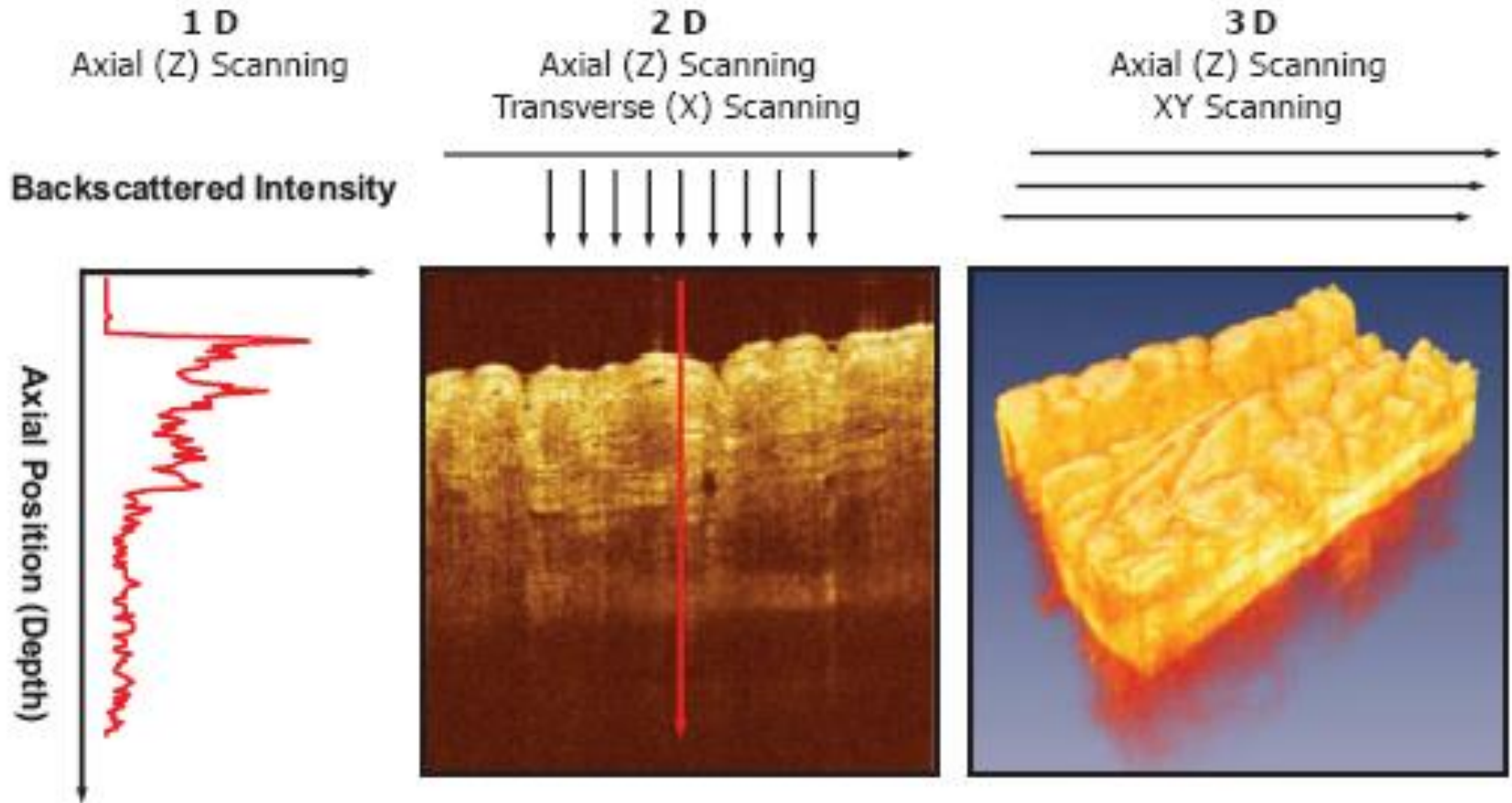
- 256 linear transducer array
- 7 mm laser focus
- Lateral resolution $140 \mu\text{m}$



1951 USAF resolution test chart, 40 MHz, 860nm



OCT: optical analogue of pulsed-wave ultrasound



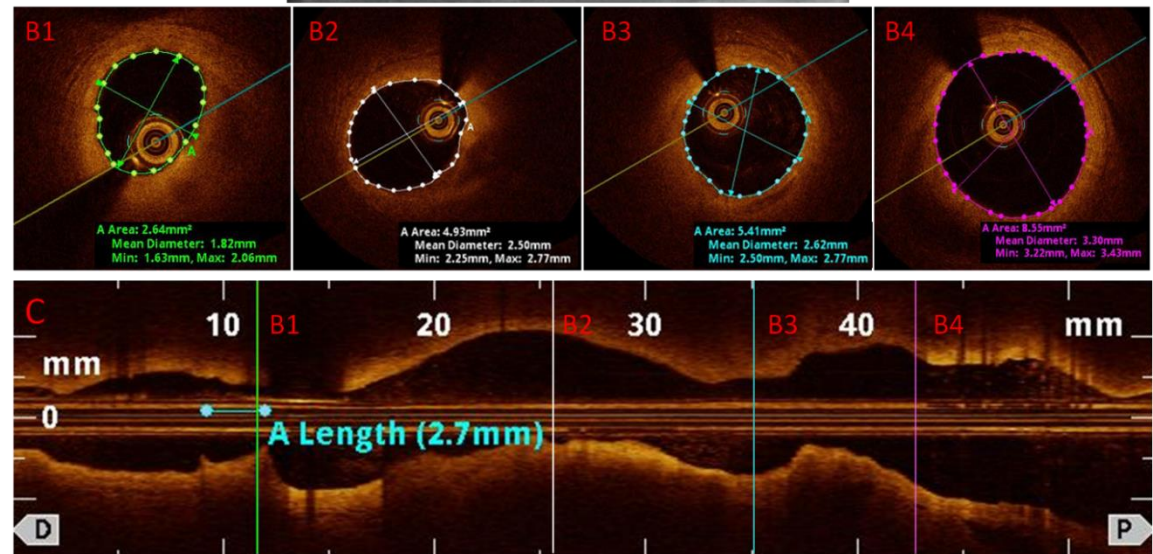
Materials & Methods



NinePoint_4.mp4

- The minimal lumen area (MLA) and minimal lumen diameter (MLD) were measured at the cross section with the smallest lumen area using FD-OCT.

- Reference lumen area (RLA) was measured at reference cross section with the largest lumen within 10 mm proximal or distal to MLA and before any side branch.

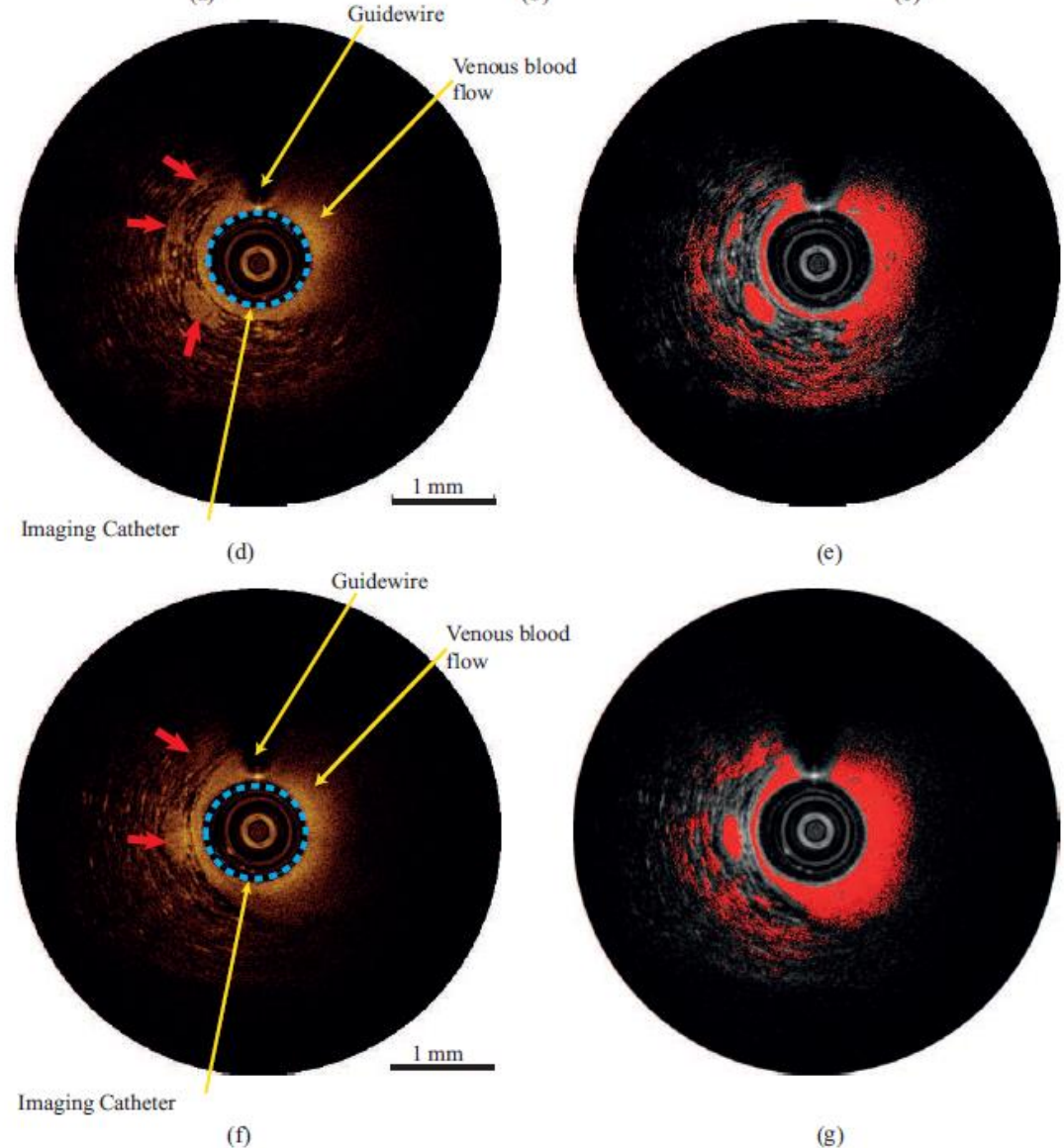
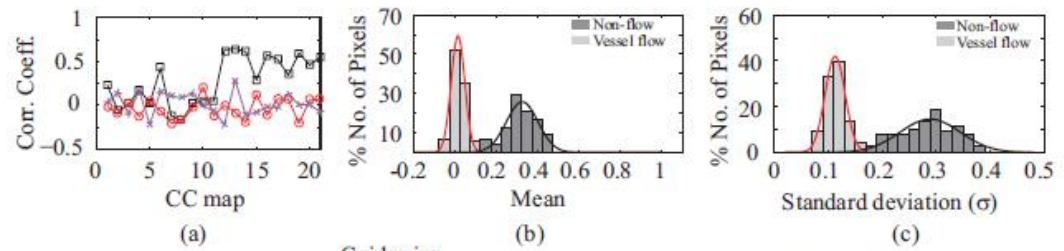


Intracoronary microcirculation

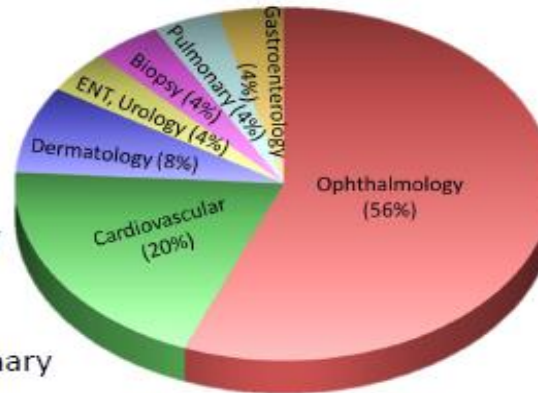
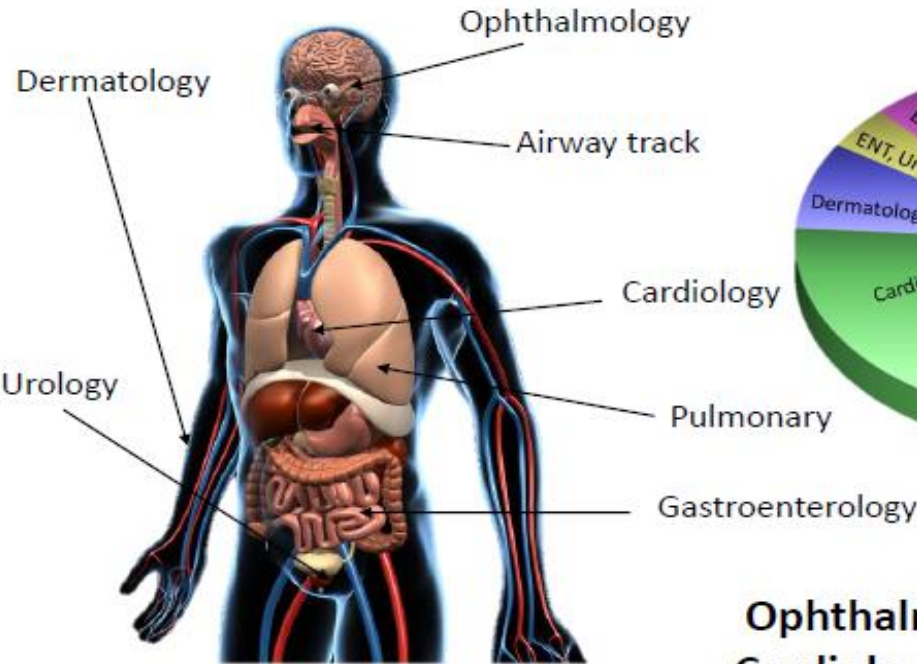
Human Coronary Sinus using the every frame CC mapping method.

(d and f) Cross-sectional OCT images obtained with zero pullback. Bold red arrows indicate the vessels. (e and g) Flow maps corresponding to (d) and (f) superimposed onto the respective OCT images.

Flow regions are marked red.



Clinical OCT Systems in the world market



~40 OCT Based Established Companies and Startups

Ophthalmology ~ 20M patients/year
 Cardiology (intravascular OCT) (~100k patients/year)

- \$6,000,000,000 in equipment sales,
 \$10,000,000,000 in health care savings.

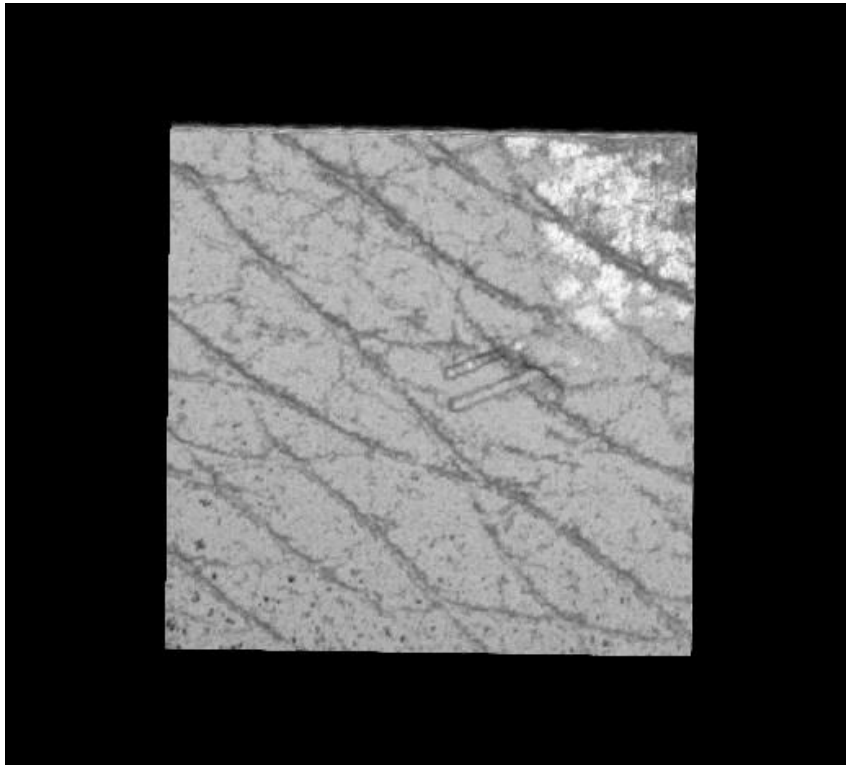
[http://www.octnews.org/articles/6849556/the-ecosystem-that-powered-the-translation-of-oct-](http://www.octnews.org/articles/6849556/the-ecosystem-that-powered-the-translation-of-oct)

[http://www.ajo.com/article/S0002-9394\(17\)30419-1/fulltext](http://www.ajo.com/article/S0002-9394(17)30419-1/fulltext)

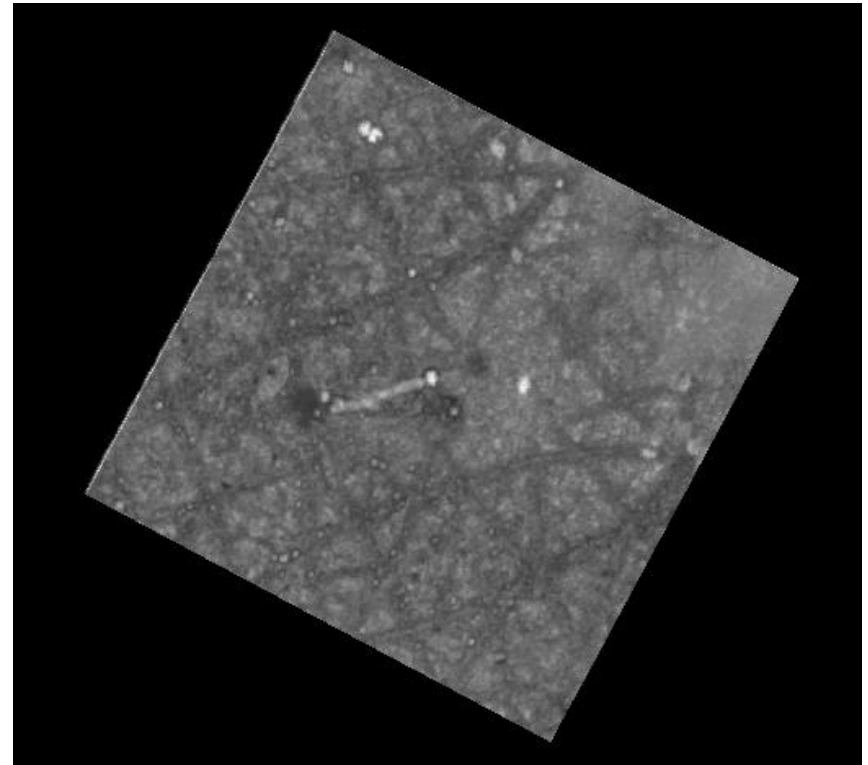


In Vivo cmOCT and Optical Clearing

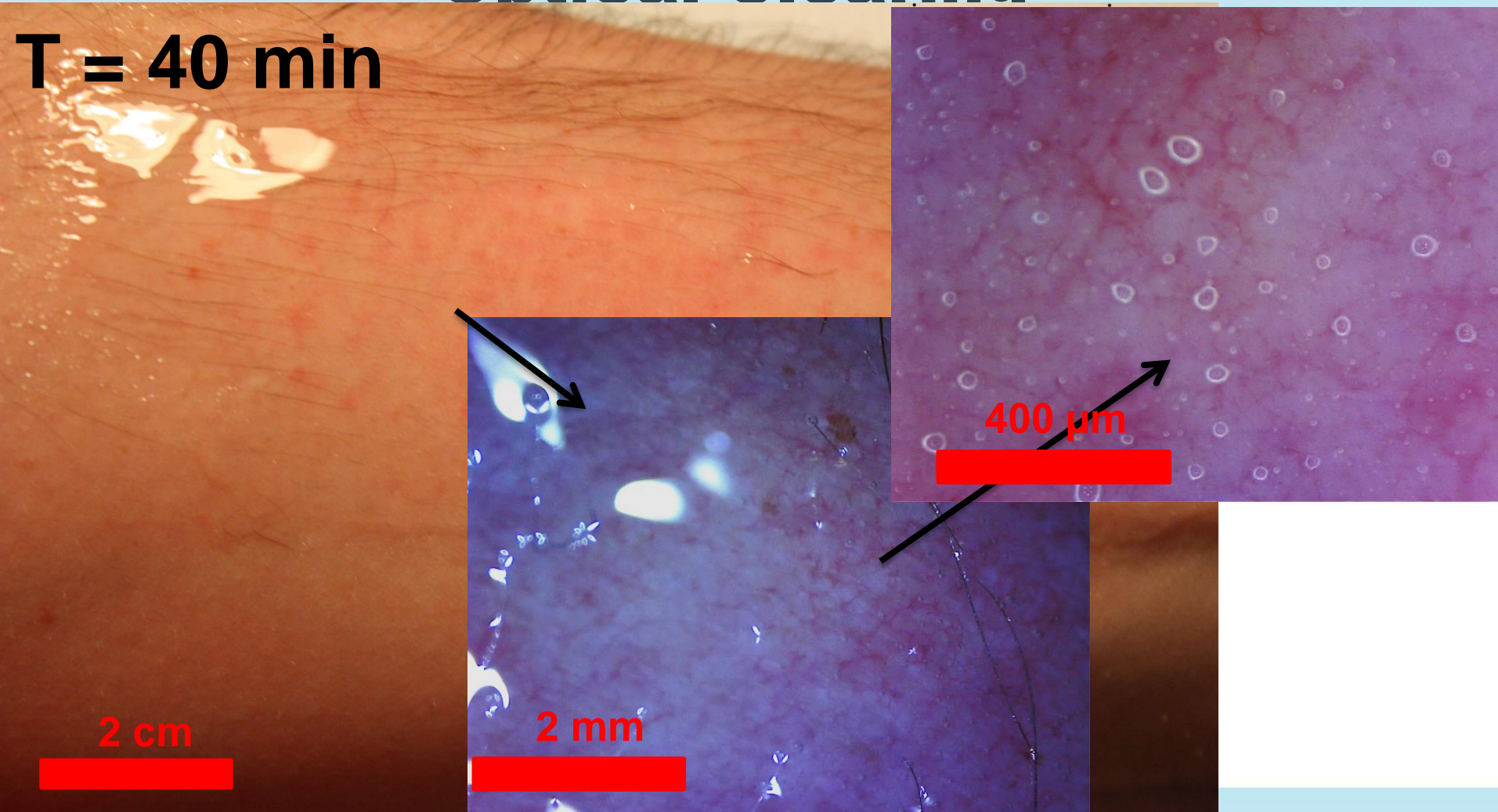
Before Clearing



After Clearing



In Vivo Human **Optical Clearing**

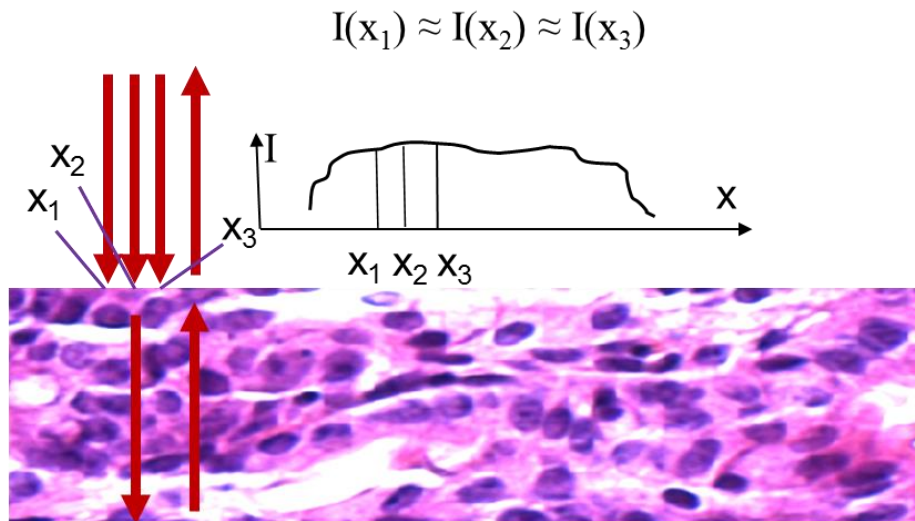


Label-free Imaging Domains

Conventional microscopy

Detector

One intensity value at each point of the image

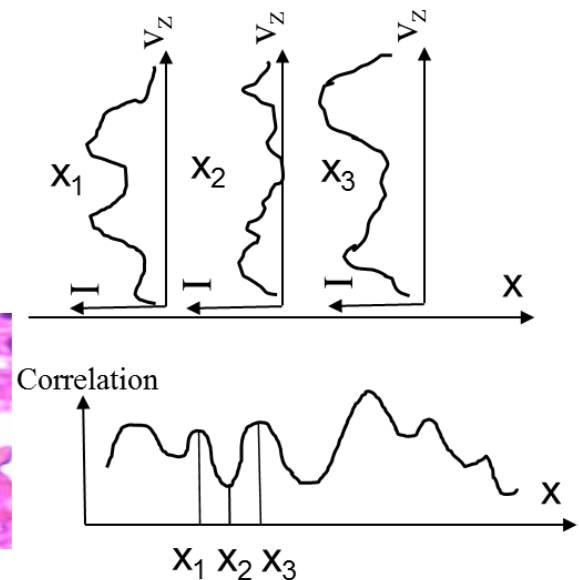


Structural features at points x_1 , x_2 , x_3 are unresolvable

srSESF microscopy

Spectral detector

Axial spatial frequency profile at each point of the image



Structural features at points x_1 , x_2 , x_3 can be resolved

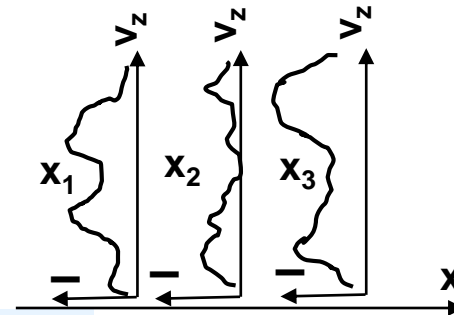
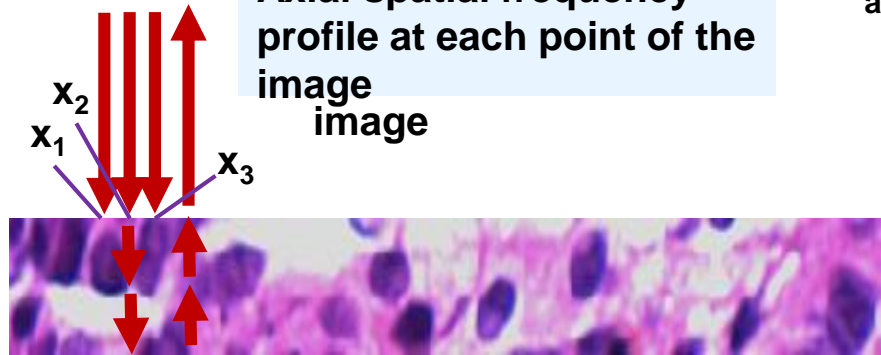


sSESF approach

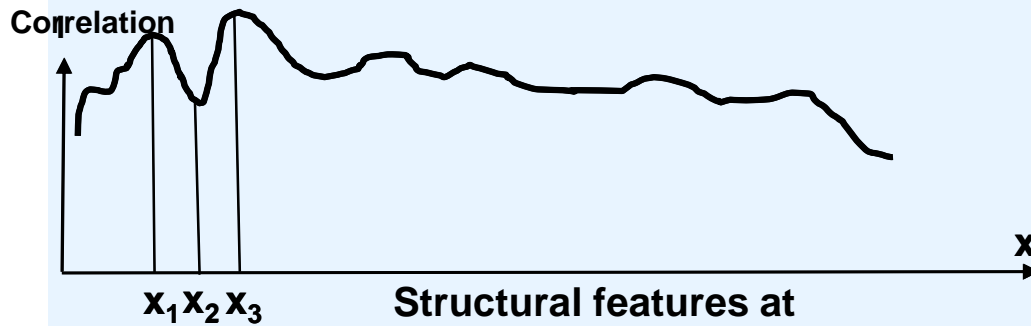
sSESF microscopy

It was shown that super-resolution image can be formed as a map of correlation between frequency profile at given point and at all other points in the image.

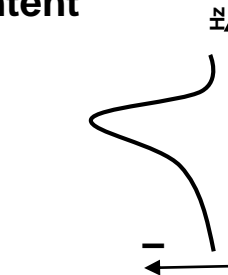
Axial spatial frequency profile at each point of the image



High frequency content



Structural features at points x_1 , x_2 , x_3 can be resolved



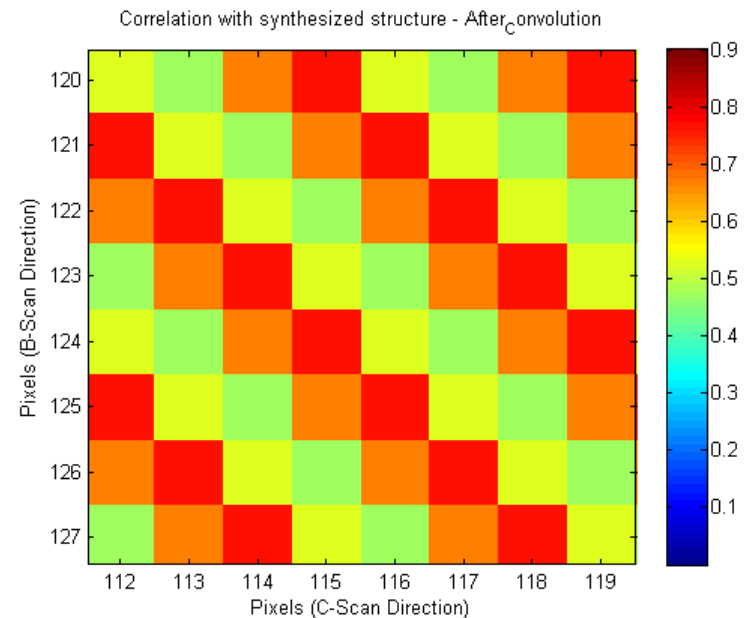
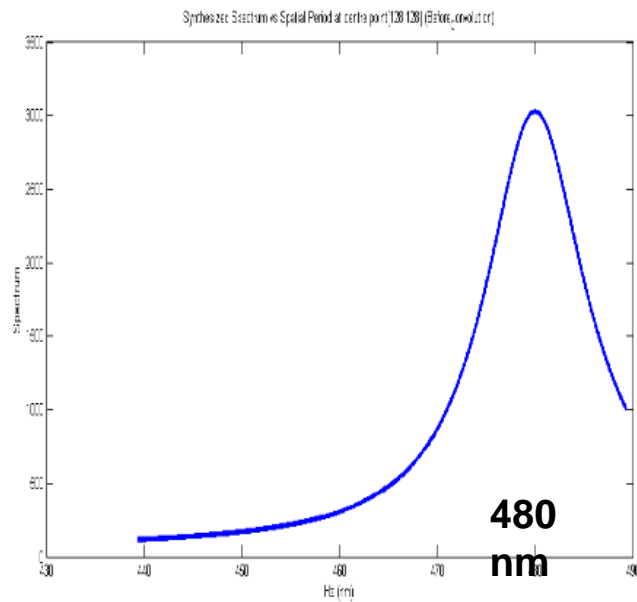
Synthesized structure



Imaging of 2D lateral structure with size beyond the diffraction resolution limit.

Size of each element of the lateral structure 600nm x 600nm, in 2 times smaller than diffraction resolution limit. Size difference in axial structure is 10 nm.

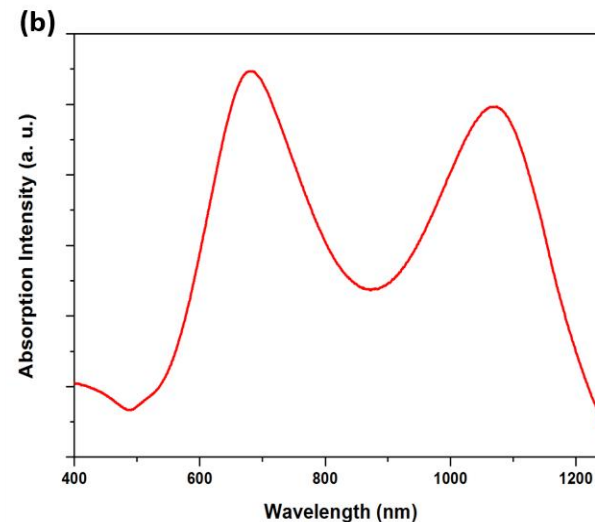
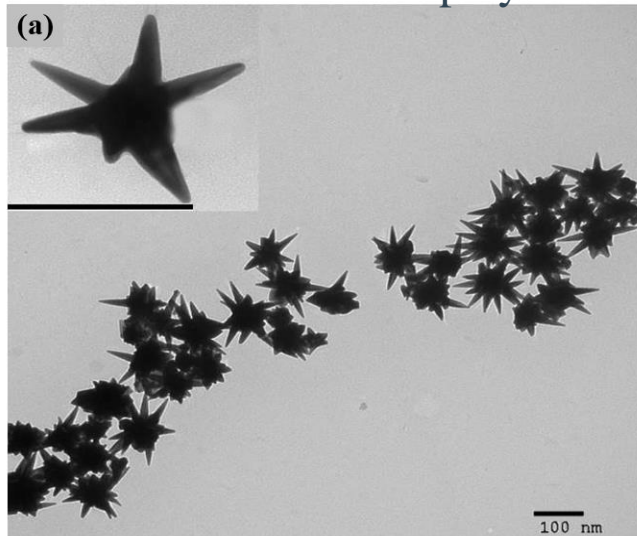
$\lambda = 1300 \text{ nm}$, $\Delta\lambda = 140 \text{ nm}$ NA = 0.5, R = 1590 nm
SNR 71 dB





Dual Plasmonic Gold NanoStars

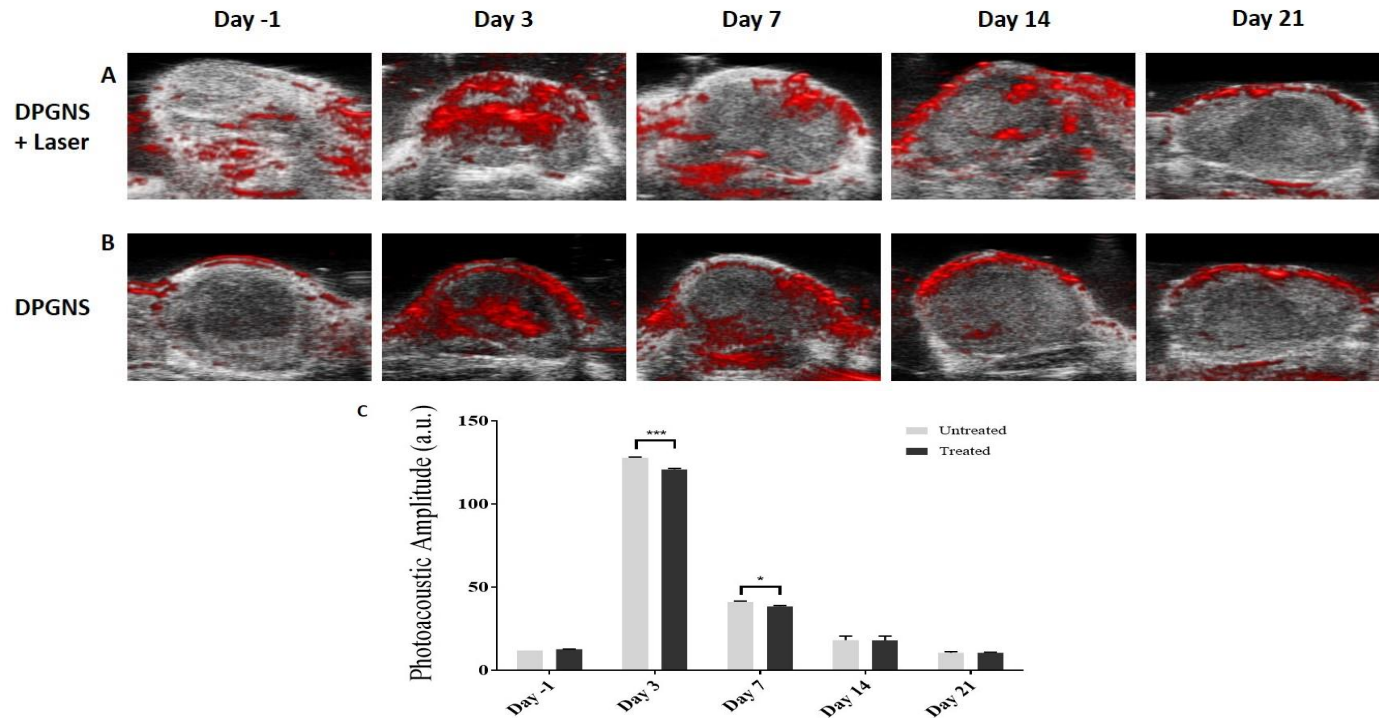
- Bimetallic configuration:
 - Silver has superior optical properties but is prone to oxidation
 - Forms FCC crystal with similar lattice constant as gold (capable of forming divisible shell geometry)
- Multibranched gold nanostars synthesised by using Ag as shape directing agents
- Synthesised nanostars displayed LSPR band in NIR



- Precursor – HAuCl_4 & Silver nitrate
- Reducing agent – Ascorbic acid

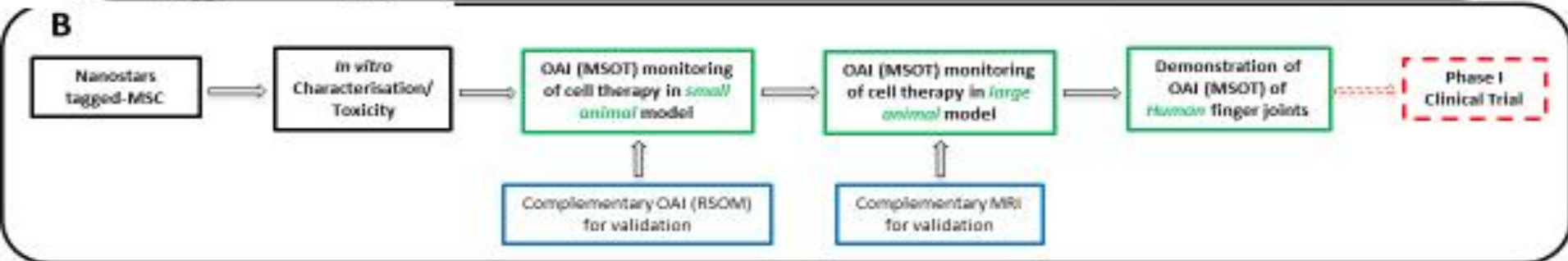
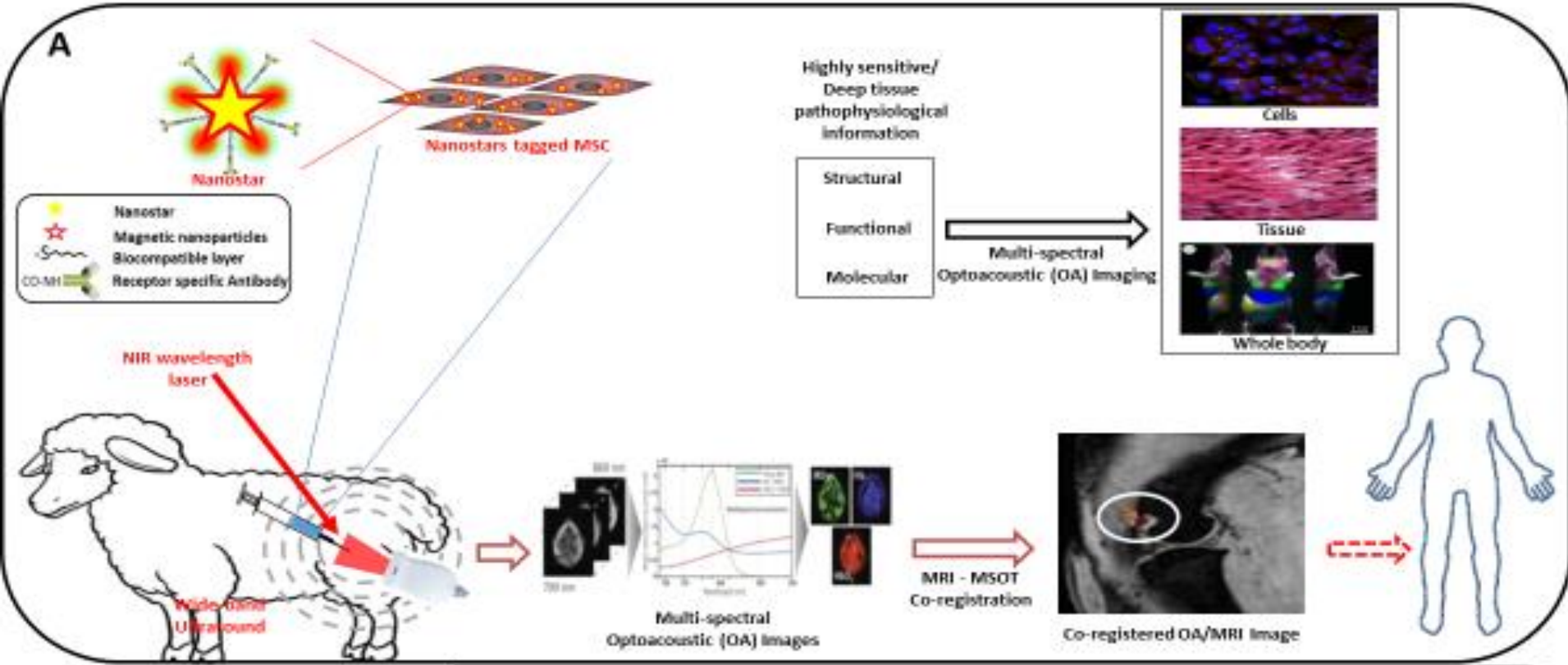


DPGNS – *In vivo* Photothermal Therapy



PA images of tumour administered with DPGNS followed by 1064 nm laser irradiation (A), tumour administered with only DPGNS (B); PA amplitude plot (C) for (A) and (B). Notice that the DPGNS retained in the tumour at Day 3 with optical properties intact even after laser exposure (0.5 W/cm² for 10 mins.)







This is our eight Biophotonics and Imaging Graduate Summer School. It is an important opportunity for graduate students in 2020 to access the kind of close contact with leading professors that only this kind of environment facilitates. Tutors for BIGSS 2020 include:

- Steve Jacques (Tufts)**- Tissue optics and modelling
- Wei Chen (Oklahoma)** – Photothermal therapy and immunology
- Paola Borri (Cardiff)**– Advanced Light Microscopy.
- Caroline Boudoux (Montreal)**– Endoscopy
- Elizabeth Hillman (Columbia)**- High-speed optical imaging and microscopy of in-vivo brain function.
- Stephen Boppart (Urbana-Champaign)**- Optical coherence tomography
- Sergio Fantini (Tufts)**- Diffuse optics and applications to tissue oximetry and non-invasive brain studies
- Brian Wilson (Dartmouth)**- Photo Medicine, Radiation Medicine and Nano Medicine
- Paul Beard + Ben Cox (London)**– Photoacoustic Imaging

<http://tomi.nuigalway.ie>; BIGSS@nuigalway.ie

Deadline: May 16th



The international society
for optics and photonics



Take away

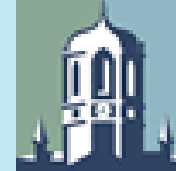
- Smallest is $1/200$ of the depth
 - BUT sensitivity to smaller is possible
- Light penetration is really about scattering
- OCT decouples width from depth resolution
- FDOCT Noise advantage

- H2020 TOPIC : Nanotechnologies for imaging cellular transplants and regenerative processes in vivo
 - €6M question

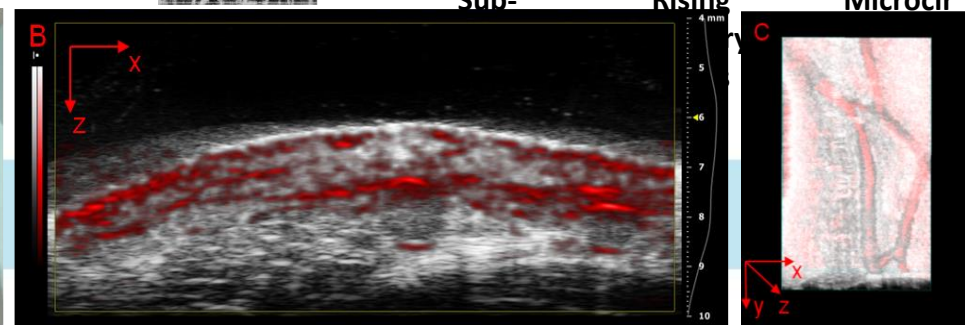
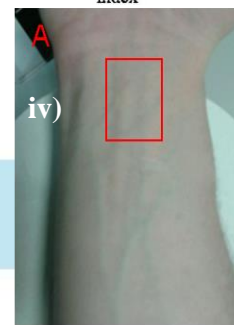
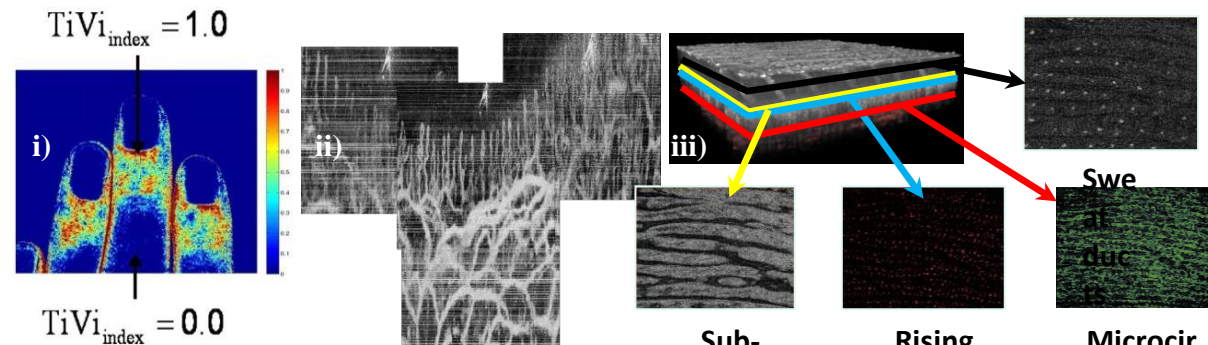
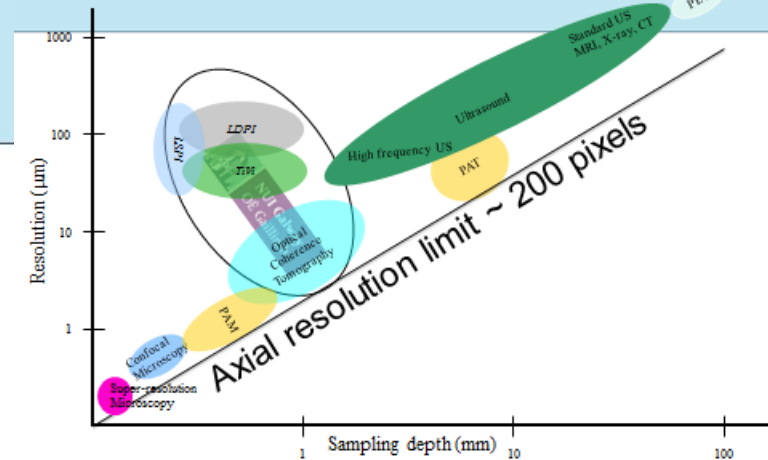


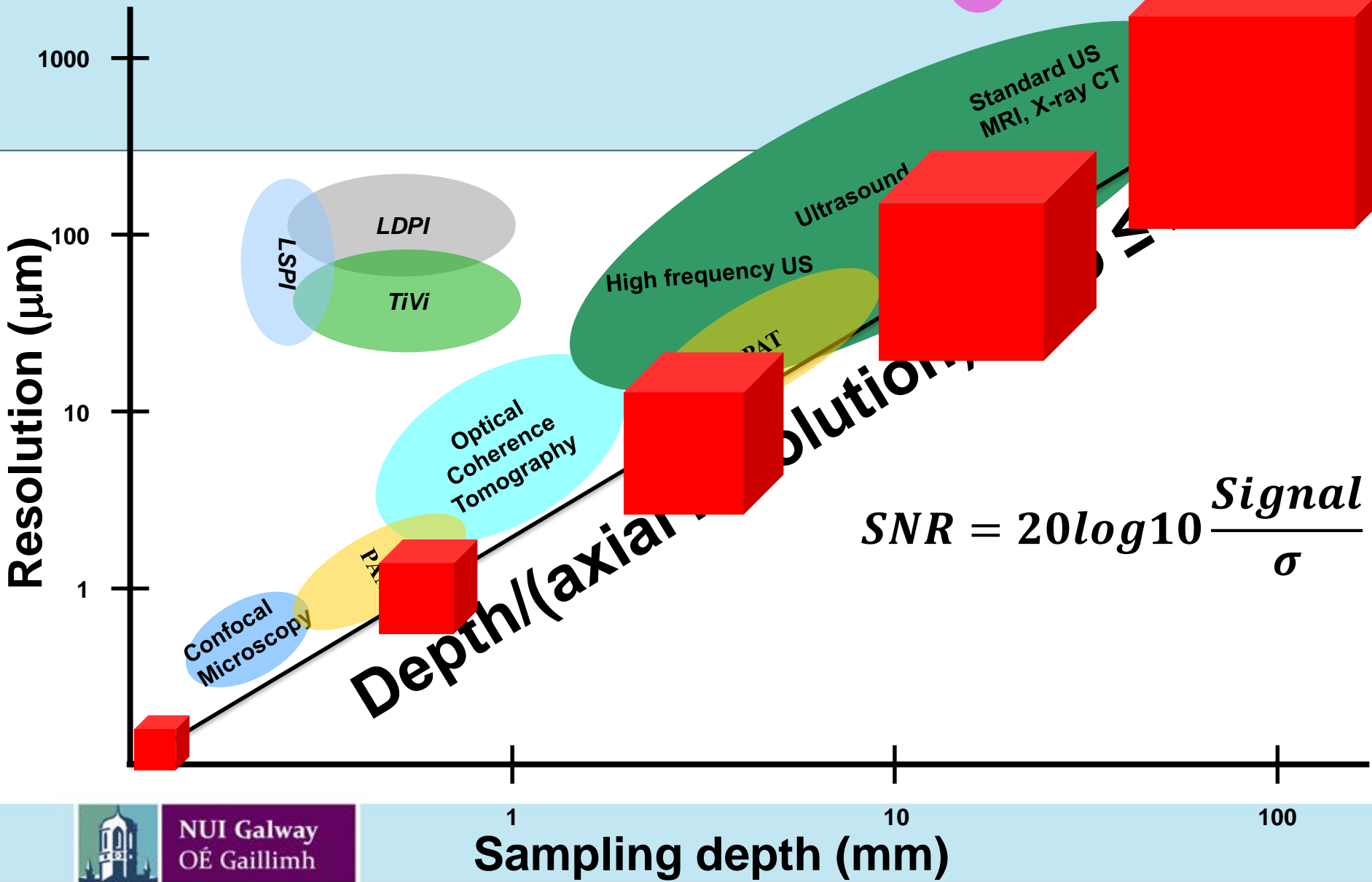
Summary

- In vivo / Ex vivo
- Scattering or non-scattering tissue?
- Depth versus resolution
- Speed – frames per second – motion?
- Functional – flow, oxygenation, molecular sensitivity
- Sub-resolution content/activity
- Fit for purpose



Imaging depth and resolution





DOT

$$SNR = 20 \log_{10} \frac{\text{Signal}}{\sigma}$$

NBIPI: Tissue Optics and Microcirculation Imaging

TOMI Team:

Head of group Prof. Martin Leahy
 Prof. Steve Jacques (adjunct)
 Prof. Valery Tuchin (adjunct)
 Dr Sergey Alexandrov
 Dr Paul McNamara
 Dr Nandan Das
 Dr Yi Zhou
 Dr Vijaya Raghavan
 Rajib Dey

Seán O’Gorman

Aedán Breathnach
 Anand Arangath
 Soorya James
 Aaron Croke

Kai Neuhaus
 Cerine Lal
 Gillian Lynch



Alumni:

Dr Jim O’Doherty, Snr. PET Physicist, King’s Hospital London
 Dr Neil Clancy, Research Fellow, Imperial College London
 Dr Joey Enfield, Senior Java Developer, Fexco
 Dr David Connolly, Assistant Professor, University of Aalborg
 Dr Anne-Marie Henihan, Research Fellow, University of Limerick
 Dr Emmanuel Pican, Lecturer ,CIT
 Dr Susan Daly, Research Fellow University of Limerick
 Dr Dennis Warncke
 Dr Paddy Finn, Crystal Energy
 Dr Paul McNamara, NUIG - Compact Imaging
 Dr Xin Gao, University of Kentucky
 Dr Marie-Louise O’Connell, Irish Medicines Board
 Dr Brian Kelleher, Lecturer, DCU
 Dr Haroon Zafar, Galway University Hospitals
 Dr Roshan Dsouza, Urbana-Champaign

Collaborators:

Fujifilm-VisualSonics, Inc.
St. Jude Medical, Inc.
Compact Imaging , Inc.
Wheelsbridge AB
iThera GmBh





This is our seventh Biophotonics and Imaging Graduate Summer School. It is an important opportunity for graduate students in 2018 to access the kind of close contact with leading professors that only this kind of environment facilitates. Tutors for BIGSS 2018 will include:

Steve Jacques (Tufts)- Tissue optics and modelling

Irving Bigio (Boston)- Nonlinear optics in spectroscopy and microscopy

Paola Borri (Cardiff)- Advanced Light Microscopy.

Caroline Boudoux (Montreal)- Endoscopy

Elizabeth Hillman (Columbia)- High-speed optical imaging and microscopy of in-vivo brain function.

Ton van Leeuwen (Amsterdam)- Optical coherence tomography

Sergio Fantini (Tufts)- Diffuse optics and applications to tissue oximetry and non-invasive brain studies

Brian Pogue (Dartmouth)- Optics in Surgery & Radiation Therapy - photochemistry/radiochemistry

Daniel Razansky (Munich)- Optoacoustic Imaging

<http://tomi.nuigalway.ie>; BIGSS@nuigalway.ie

Deadline: May 16th



The international society
for optics and photonics

